References

Bagrodia S, Derijard B, Davis RJ, Cerione RA. (1995). *J Biol Chem* **270**: 27995–27998.
Bazenet CE, Mota MA, Rubin LL. (1998). *Proc Natl Acad Sci USA* **95**: 3984–3989.
Boyd JM, Malstrom S, Subramanian T, Venkatesh LK, Schaeper U, Elangovan B *et al.* (1994). *Cell* **79**: 341–351.
Brodeur GM, Pritchard J, Berthold F, Carlsen NL, Castel V, Castelberry RP *et al.* (1993). *J Clin Oncol* **11**: 1466–1477.
Brodeur GM, Seeger RC, Schwab M, Varmus HE, Bishop JM. (1984). *Science* **224**: 1121–1124.
Burge C, Karlin S. (1997). *J Mol Biol* **268**: 78–94.
Burge CB, Karlin S. (1998). *Curr Opin Struct Biol* **8**: 346–354.
Cahill MA, Peter ME, Kischkel FC, Chinnaiyan AM, Dixit VM, Krammer PH *et al.* (1996). *Oncogene* **13**: 2087–2096.
Caron H. (1995). *Med Pediatr Oncol* **24**: 215–221.
Chuang TH, Hahn KM, Lee JD, Danley DE, Bokoch GM. (1997). *Mol Biol Cell* **8**: 1687–1698.
Coso OA, Chiariello M, Yu JC, Teramoto H, Crespo P, Xu N *et al.* (1995). *Cell* **81**: 1137–1146.
Evans AE, Gerson J, Schnaufer L. (1976). *Natl Cancer Inst Monogr* **44**: 49–54.
Favrot MC, Combaret V, Lasset C. (1993). *N Engl J Med* **329**: 1965.
Garcia I, Martinou I, Tsujimoto Y, Martinou JC. (1992). *Science* **258**: 302–304.
Garnier M, Di Lorenzo D, Albertini A, Maggi A. (1997). *J Neurosci* **17**: 4591–4599.
Gjoerup O, Lukas J, Bartek J, Willumsen BM. (1998). *J Biol Chem* **273**: 18812–18818.
Gooding LR, Aquino L, Duerksen-Hughes PJ, Day D, Horton TM, Yei SP *et al.* (1991). *J Virol* **65**: 3083–3094.
Hashimoto S, Ishii A, Yonehara S. (1991). *Int Immunol* **3**: 343–351.
Hockenbery D, Nunez G, Milliman C, Schreiber RD, Korsmeyer SJ. (1990). *Nature* **348**: 334–336.
Horton P, Nakai K. (1996). *Proc Int Conf Intell Syst Mol Biol* **4**: 109–115.
Islam A, Kageyama H, Takada N, Kawamoto T, Takayasu H, Isogai E *et al.* (2000). *Oncogene* **19**: 617–623.
Juo P, Kuo CJ, Reynolds SE, Konz RF, Raingeaud J, Davis RJ *et al.* (1997). *Mol Cell Biol* **17**: 24–35.
Kaneko M, Nishihira H, Mugishima H, Ohnuma N, Nakada K, Kawa K *et al.* (1998). *Med Pediatr Oncol* **31**: 1–7.
Kozak M. (1987). *Nucl Acids Res* **15**: 8125–8148.
Larisch S, Yi Y, Lotan R, Kerner H, Eimerl S, Tony Parks W *et al.* (2000). *Nat Cell Biol* **2**: 915–921.
Lee VM, Shelanski ML, Greene LA. (1980). *Neuroscience* **5**: 2239–2245.
Lenczowski JM, Dominguez L, Eder AM, King LB, Zacharchuk CM, Ashwell JD. (1997). *Mol Cell Biol* **17**: 170–181.
Low BC, Seow KT, Guy GR. (2000). *J Biol Chem* **275**: 37742–37751.
Moasser MM, Khoo KS, Maerz WJ, Zelenetz A, Dmitrovsky E. (1996). *Differentiation* **60**: 251–257.
Nagai M, Ichimiya S, Ozaki T, Seki N, Mihara M, Furuta S *et al.* (2000). *Int J Oncol* **16**: 907–916.
Nakagawara A. (1998). *Hum Cell* **11**: 115–124.
Nakagawara A. (2001). *Cancer Lett* **169**: 107–114.
Nakagawara A, Arima-Nakagawara M, Scavarda NJ, Azar CG, Cantor AB, Brodeur GM. (1993). *N Engl J Med* **328**: 847–854.
Nakagawara A, Azar CG, Scavarda NJ, Brodeur GM. (1994). *Mol Cell Biol* **14**: 759–767.
Nakagawara A, Milbrandt J, Muramatsu T, Deuel TF, Zhao H, Cnaan A *et al.* (1995). *Cancer Res* **55**: 1792–1797.
Nakamura Y, Ozaki T, Ichimiya S, Nakagawara A, Sakiyama S. (1998). *Biochem Biophys Res Commun* **243**: 722–726.
Ohira M, Morohashi A, Inuzuka H, Shishikura T, Kawamoto T, Kageyama H *et al.* (2003a). *Oncogene* **22**: 5525–5536.
Ohira M, Morohashi A, Nakamura Y, Isogai E, Furuya K, Hamano S *et al.* (2003b). *Cancer Lett* **197**: 63–68.
Olson MF, Ashworth A, Hall A. (1995). *Science* **269**: 1270–1272.
Oltvai ZN, Milliman CL, Korsmeyer SJ. (1993). *Cell* **74**: 609–619.
Seimiya H, Mashima T, Toho M, Tsuruo T. (1997). *J Biol Chem* **272**: 4631–4636.
Shimada H, Chatten J, Newton Jr WA, Sachs N, Hamoudi AB, Chiba T *et al.* (1984). *J Natl Cancer Inst* **73**: 405–416.
Solovyev VV, Salamov AA. (1999). *Nucl Acids Res* **27**: 248–250.
Subramanian T, Boyd JM, Chinnadurai G. (1995). *Oncogene* **11**: 2403–2409.
Takihara Y, Tomotsune D, Shirai M, Katoh-Fukui Y, Nishii K, Motaleb MA *et al.* (1997). *Development* **124**: 3673–3682.
Tanaka T, Sugimoto T, Sawada T. (1998). *Cancer* **83**: 1626–1633.
Vegeto E, Pollio G, Pellicciari C, Maggi A. (1999). *FASEB J* **13**: 793–803.
White E, Sabbatini P, Debbas M, Wold WS, Kusher DI, Gooding LR. (1992). *Mol Cell Biol* **12**: 2570–2580.
Whitfield J, Neame SJ, Paquet L, Bernard O, Ham J. (2001). *Neuron* **29**: 629–643.
Yamamoto M, Marui N, Sakai T, Morii N, Kozaki S, Ikai K *et al.* (1993). *Oncogene* **8**: 1449–1455.
Yuan J, Horvitz HR. (1992). *Development* **116**: 309–320.
Zhang B, Zhang Y, Collins CC, Johnson DI, Zheng Y. (1999). *J Biol Chem* **274**: 2609–2612.
Zhang B, Zheng Y. (1998). *J Biol Chem* **273**: 25728–25733.
Zhang S, Han J, Sells MA, Chernoff J, Knaus UG, Ulevitch RJ *et al.* (1995). *J Biol Chem* **270**: 23934–23936.
Zhou YT, Soh UJ, Shang X, Guy GR, Low BC. (2002). *J Biol Chem* **277**: 7483–7492.
Zou H, Henzel WJ, Liu X, Lutschg A, Wang X. (1997). *Cell* **90**: 405–413.

Oncogene (2006) 25, 5046–5055

www.nature.com/onc

ORIGINAL ARTICLE

Bcl-2 is a key regulator for the retinoic acid-induced apoptotic cell death in neuroblastoma

H Niizuma[1,2], Y Nakamura[1], T Ozaki[1], H Nakanishi[1], M Ohira[1], E Isogai[1], H Kageyama[1], M Imaizumi[3] and A Nakagawara[1]

[1]Division of Biochemistry, Chiba Cancer Center Research Institute, Chuoh-ku, Chiba, Japan; [2]Department of Pediatrics, Tohoku University School of Medicine, Aoba-ku, Sendai, Japan and [3]Department of Hematology and Oncology, Miyagi Children's Hospital, Aoba-ku, Sendai, Japan

Retinoic acid (RA) has been shown to induce neuronal differentiation and/or apoptosis, and is widely used as a chemotherapeutic agent for treating the patients with neuroblastoma. However, the therapeutic effect of RA is still limited. To unveil the molecular mechanism(s) inducing differentiation and apoptosis in neuroblastoma cells, we compared CHP134 and NB-39-nu cell lines, in which all-*trans*-RA (ATRA) induces apoptosis, with LA-N-5 and RTBM1 cell lines, in which it induces neuronal differentiation. Here, we found that Bcl-2 was strongly downregulated in CHP134 and NB-39-nu cells, whereas it was abundantly expressed in LA-N-5 and RTBM1 cells. ATRA-mediated apoptosis in CHP134 and NB-39-nu cells was associated with a significant activation of caspase-9 and caspase-3 as well as cytoplasmic release of cytochrome *c* from mitochondria in a p53-independent manner. Enforced expression of Bcl-2 significantly inhibited ATRA-mediated apoptosis in CHP134 cells. In addition, treatment of RTBM1 cells with a Bcl-2 inhibitor, HA14-1, enhanced apoptotic response induced by ATRA. Of note, two out of 10 sporadic neuroblastomas expressed *bcl-2* at undetectable levels and underwent cell death in response to ATRA in primary cultures. Thus, our present results suggest that overexpression of Bcl-2 is one of the key mechanisms to give neuroblastoma cells the resistance against ATRA-mediated apoptosis. This may provide a new therapeutic strategy against the ATRA-resistant and aggressive neuroblastomas by combining treatment with ATRA and a Bcl-2 inhibitor.
Oncogene (2006) **25**, 5046–5055. doi:10.1038/sj.onc.1209515; published online 27 March 2006

Keywords: apoptosis; Bcl-2; neuroblastoma; retinoic acid

Correspondence: Dr A Nakagawara, Division of Biochemistry, Chiba Cancer Center Research Institute, 666-2 Nitona, Chuoh-ku, Chiba 260-8717, Japan.
E-mail: akiranak@chiba-cc.jp
Received 8 November 2005; revised 6 February 2006; accepted 15 February 2006; published online 27 March 2006

Introduction

Neuroblastoma, which originates from the sympathoadrenal lineage of the neural crest, is one of the most common solid tumors in childhood and has distinct biological properties in different prognostic subsets (Schor, 1999). For example, tumors in patients less than 1 year of age often regress spontaneously and have a favorable prognosis. In contrast, tumors that occur over 1 year of age display an extensive and metastatic disease at diagnosis, and are often aggressive with an unfavorable prognosis despite an intensive therapy (Brodeur and Nakagawara, 1992). Each of those subsets shows various distinct genetic features including the ploidy status, *MYCN* amplification, allelic loss of the distal part of chromosome 1p and the gain of chromosome 17q (Brodeur, 2003). Additionally, high expression levels of neurotrophin receptors TrkA and TrkB are favorable and unfavorable prognostic indicators of neuroblastomas, respectively (Nakagawara *et al.*, 1993, 1994). Several lines of evidence suggest that the spontaneous regression of the favorable neuroblastomas is attributed at least in part to the developmentally programmed neuronal cell death and/or neuronal differentiation (Nakagawara, 1998). Indeed, the deprivation of nerve growth factor led to the massive cell death through apoptosis of neuroblastoma cells expressing TrkA (Nakagawara *et al.*, 1993).

Retinoic acids (RAs), which appear to be involved in vertebrate morphogenesis, are natural and synthetic derivatives of vitamin A (Maden, 2001; McCaffery *et al.*, 2003), and exert their biological functions through nuclear receptors including RA receptors (RARs) and retinoid X receptors (RXRs) (Lippman and Lotan, 2000). In response to RA binding, RAR/RXR heterodimers regulate the transcription of a number of target genes by binding to the specific DNA response elements (Balmer and Blomhoff, 2002). Retinoic acids have antitumor effects on neuroblastoma-derived cell lines accompanied by a marked decrease in the expression levels of *MYCN* (Thiele *et al.*, 1985). Studies utilizing cell lines also have revealed that neuroblastoma cell lines exposed to all-*trans*-RA (ATRA) undergo neuronal differentiation, cell cycle arrest and/or apoptosis (Melino *et al.*, 1997; van Noesel and Versteeg, 2004). Recent

works offer insights into the molecular mechanisms by which ATRA exerts its biological effects on neuroblastomas. All-*trans*-retinoic acid activates phosphatidylinositol 3′-kinase-Akt pathway that plays an important role in neuronal differentiation (Encinas *et al.*, 1999; Lopez-Carballo *et al.*, 2002), and it reduces the expression levels of MYCN (Thiele *et al.*, 1985) and upregulates the cyclin-dependent kinase (CDK) inhibitor $p27^{KIP1}$ in association with the ATRA-induced cell cycle arrest in neuroblastoma cells (Lee *et al.*, 1996; Nakamura *et al.*, 2003). In addition, certain neuroblastoma cells underwent apoptosis in response to ATRA (Piacentini *et al.*, 1992; Takada *et al.*, 2001; Nagai *et al.*, 2004). Consistent with these observations, 13-*cis*-RA treatment after intensive chemotherapy improved an event-free survival rate of the patients with aggressive neuroblastomas with 17% increase (Villablanca *et al.*, 1995; Matthay *et al.*, 1999). Although the antitumor effects of RA alone on aggressive neuroblastoma are limited, RA treatment has an advantage that it carries no severe side effects. Thus, it is important to enhance the antitumor effects of RA on neuroblastoma cells, and thereby inducing apoptosis.

In the present study, we have found that the ATRA treatment induces neuronal differentiation in neuroblastoma-derived LA-N-5 and RTBM1 cells, whereas CHP134 and NB-39-nu cells undergo p53-independent apoptotic cell death in response to ATRA. Extensive expression studies revealed that the antiapoptotic Bcl-2 was constitutively expressed at high levels in LA-N-5 and RTBM1 cells, whereas CHP134 and NB-39-nu cells expressed Bcl-2 at extremely low levels. Enforced expression of Bcl-2 in CHP134 cells led to a significant inhibition of the ATRA-mediated apoptosis. In accordance with these results, the treatment with Bcl-2 inhibitor in RTBM1 cells resulted in an increased sensitivity to ATRA. Moreover, two out of 10 sporadic neuroblastomas in primary cultures with undetectable *bcl-2* underwent cell death in response to ATRA, whereas seven tumors out of the remaining eight cases expressed high levels of *bcl-2*. These results suggest that Bcl-2 might be a key regulator for the ATRA-mediated apoptotic cell death in neuroblastomas.

Results

ATRA-induced growth inhibition, differentiation and cell death in human neuroblastoma cell lines

To examine the possible effects of ATRA on growth and viability of neuroblastoma cells, human neuroblastoma-derived LA-N-5, RTBM1, CHP134 and NB-39-nu cells were cultured with or without 5 μM of ATRA, and the numbers of viable cells were counted at the indicated time points after the exposure to ATRA. As shown in Figure 1a, ATRA effectively inhibited proliferation of these neuroblastoma cells. Among them, the growth of CHP134 and NB-39-nu cells was much more suppressed in the presence of ATRA. To monitor morphological changes induced by ATRA, ATRA-treated cells were checked by phase-contrast microscopy. As shown in Figure 1b, a neurite outgrowth was evident in ATRA-treated LA-N-5, RTBM1 and CHP134 cells, whereas it was marginal in NB-39-nu cells. Of note, ATRA-induced cell death was detectable in CHP134 and NB-39-nu cells, but not in LA-N-5 and RTBM1 cells. To confirm whether ATRA could induce the apoptotic cell death in CHP134 and NB-39-nu cells, we examined the changes in the number of cells with sub-G1 DNA content in response to ATRA. As shown in Figure 1c and d, the flow cytometric analysis revealed that the number of CHP134 cells with sub-G1 DNA content was significantly increased in response to ATRA. Similarly, ATRA promoted the apoptotic cell death in NB-39-nu cells, albeit to a lesser degree than CHP134 cells. Under our experimental conditions, ATRA failed to induce the apoptotic cell death in LA-N-5 and RTBM1 cells (data not shown).

ATRA-induced apoptotic cell death in neuroblastoma cells

To elucidate the molecular mechanism(s) underlying the ATRA-mediated apoptotic cell death in neuroblastoma cells, we examined whether the procaspases could be proteolytically cleaved to be activated in response to ATRA. To this end, whole-cell lysates prepared from the indicated neuroblastoma cells exposed to 5 μM of ATRA for 0, 2, 4 and 6 days were subjected to immunoblotting with the indicated antibodies. As shown in Figure 2a, the time-dependent proteolytic cleavage of caspase-9 and caspase-3 was observed in CHP134 and NB-39-nu cells, but not in LA-N-5 and RTBM1 cells. Consistent with these results, one of the physiological substrates of the activated caspase-3, poly-ADP-ribose polymerase (PARP), was cleaved in ATRA-treated CHP134 and NB-39-nu cells. In a good agreement with the previous observations showing that caspase-8 is epigenetically silenced in a high percentage of neuroblastoma cells (Teitz *et al.*, 2000; van Noesel *et al.*, 2003), caspase-8 was undetectable in LA-N-5, RTBM1 and CHP134 cells. In contrast, NB-39-nu cells expressed a large amount of procaspase-8. Procaspase-12, which is involved in the endoplasmic reticulum-stress-induced apoptosis (Nakagawa *et al.*, 2000; Morishima *et al.*, 2002), was readily detectable in all of the neuroblastoma cell lines that we examined, and did not respond to ATRA. Under our experimental conditions, ATRA had negligible effects on proteolytic cleavage of caspase-8 and caspase-12 (data not shown).

As caspase-9 is activated in response to the cytoplasmic release of cytochrome *c* from mitochondria, leading to the activation of caspase-3 (Degterev *et al.*, 2003), we sought to examine whether cytochrome *c* could be released in response to ATRA. To this end, CHP134 cells were treated with 5 μM of ATRA or left untreated, and cells were incubated with the antibody against cytochrome *c* or with the control immunoglobulin (Ig)G. Cell nuclei were stained with 4,6-diamidino-2-phenylindole (DAPI). Microscopic images demonstrated that cytochrome *c* staining displays a punctuate

cytoplasmic pattern in the absence of ATRA (Figure 2b, left). This staining pattern was almost identical to the MitoTracker staining (data not shown). ATRA treatment for 4 days induced redistribution of cytochrome *c* to a diffused cytoplasmic pattern in cells with apoptotic nuclei (Figure 2b, middle), suggesting

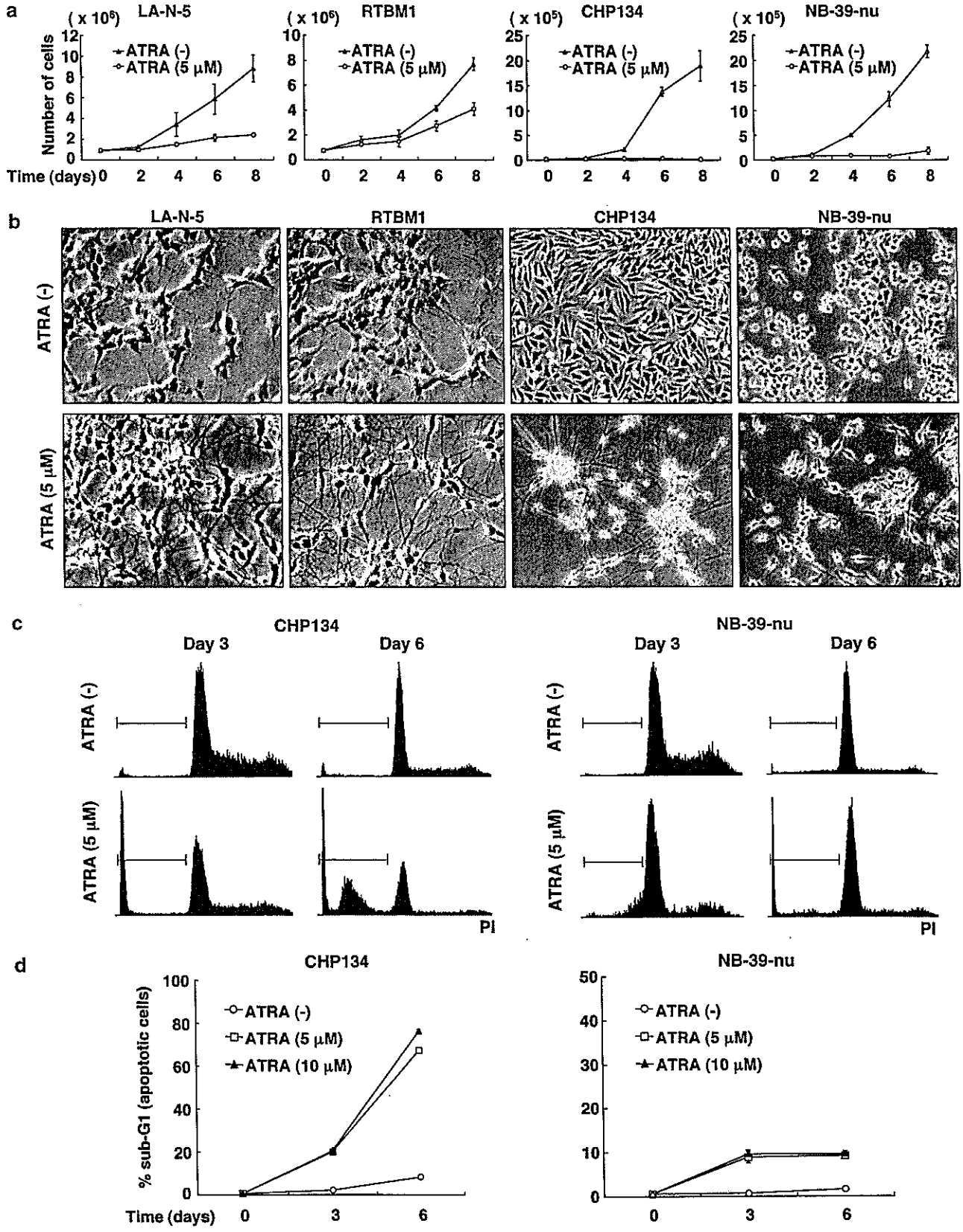

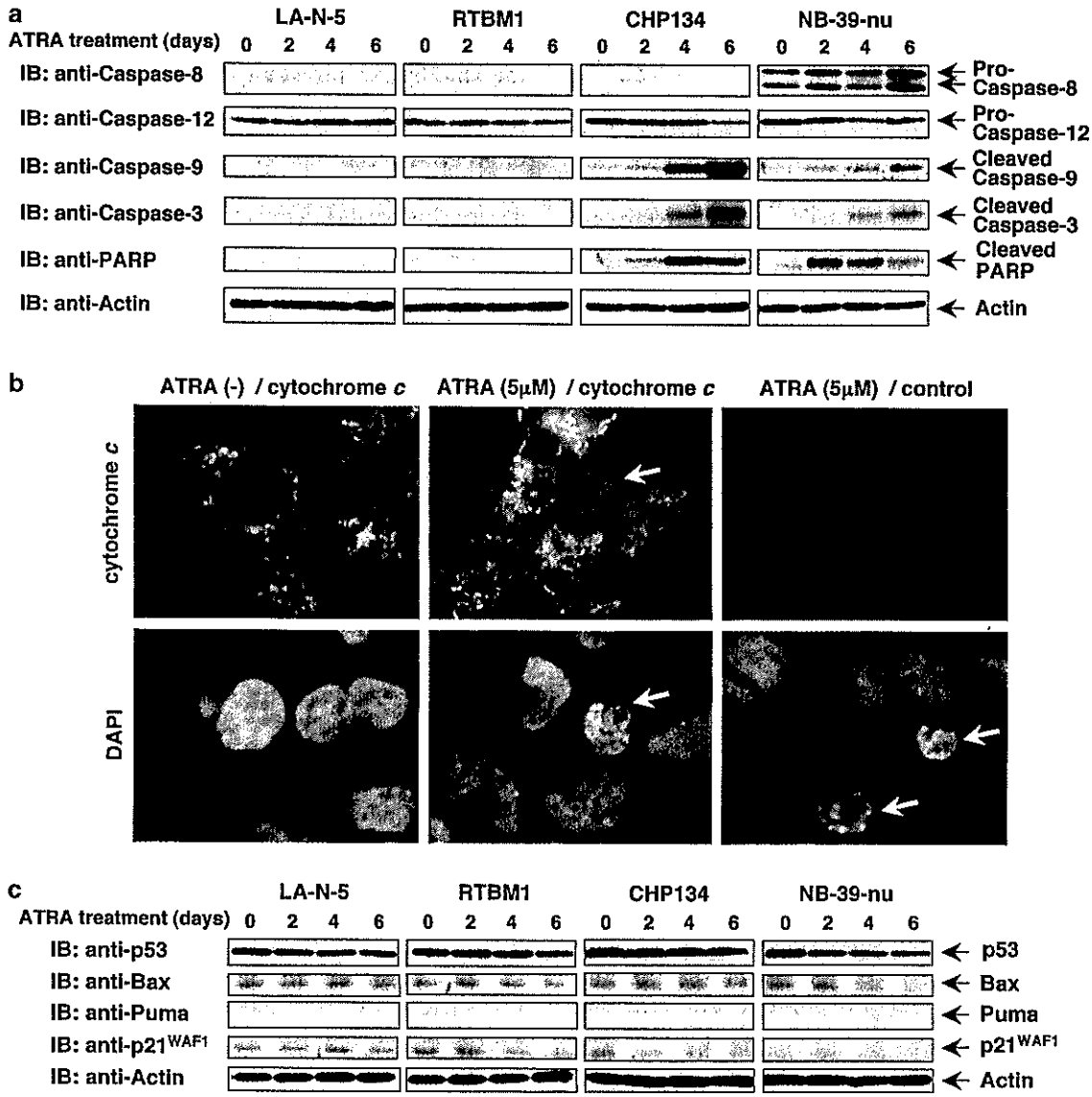

Figure 2 Caspase-9 and caspase-3 are cleaved during the all-*trans* retinoic acid (ATRA)-mediated apoptosis in CHP134 and NB-39-nu cells. (a) Immunoblot analysis for various caspases and poly-ADP-ribose polymerase (PARP) in response to ATRA. The indicated neuroblastoma cell lines were treated with 5 μM of ATRA or left untreated. At the indicated time points after the treatment with ATRA, whole-cell lysates were prepared, and analysed by immunoblotting with indicated antibodies. Actin expression was used as a loading control (bottom). (b) ATRA-induced cytoplasmic release of cytochrome *c* in CHP134 cells. CHP134 cells were seeded onto coverslips, and cultured in the presence or absence of 5 μM of ATRA. Four days after the treatment with ATRA, cells were fixed and stained with a monoclonal antibody against cytochrome *c* (top, left and middle) or with a normal mouse IgG (top, right). The cell nuclei were stained with 4,6-diamidino-2-phenylindole (DAPI) (bottom). The arrows indicate apoptotic cells with condensed and fragmented nuclei. (c) Expression levels of p53 and its direct target gene products in response to ATRA. At the indicated time periods after the treatment with ATRA, whole-cell lysates were prepared, and subjected to immunoblotting with antibodies against p53, Bax, Puma, $p21^{WAF1}$ and actin. Immunoblotting for actin is shown as a control for protein loading (bottom).

Figure 1 Effects of all-*trans* retinoic acid (ATRA) on cell proliferation of LA-N-5, RTBM1, CHP134 and NB-39-nu neuroblastoma-derived cell lines. (a) Growth curves of the indicated neuroblastoma cell lines in the presence or absence of ATRA. Cells were grown in the standard culture medium, and treated with 5 μM of ATRA. At the indicated time points after the treatment with ATRA, cells were trypsinized, harvested and number of viable cells was counted in triplicate. (b) ATRA-induced morphological changes of neuroblastoma cell lines. Cells were exposed to ATRA at a final concentration of 5 μM or left untreated. Six days after the treatment with ATRA, cells were examined by phase-contrast microscopy. (c and d) ATRA-induced cell death through apoptosis in CHP134 and NB-39-nu cells. Cells were treated with the indicated concentrations of ATRA or left untreated, and incubated for up to 6 days. At the indicated time points after the treatment with ATRA, cells were collected, fixed and stained with propidium iodide (PI). The DNA content of the cells was then examined by flow cytometry (c). The number of cells with sub-G1 DNA content was counted in triplicate (d).

that cytochrome *c* release from mitochondria might play an important role in ATRA-induced apoptotic cell death in neuroblastoma cells.

As the neuroblastoma cell lines that we examined carry wild-type p53 (data not shown), we investigated whether p53 could contribute to the ATRA-mediated apoptotic cell death. For this purpose, whole-cell lysates prepared from the indicated neuroblastoma cells exposed to 5 μM of ATRA for 0, 2, 4 and 6 days were processed for immunoblotting with the indicated antibodies. As shown in Figure 2c, the amounts of p53 remained unchanged or slightly decreased after ATRA treatment. In accordance with these results, ATRA had undetectable effects on the expression levels of p53-responsible Bax, Puma and $p21^{WAF1}$, which are implicated in the p53-dependent apoptosis and/or cell cycle arrest (Culmsee and Mattson, 2005). In addition, ATRA failed to induce the phosphorylation of p53 at Ser-15 (data not shown). Thus, it is likely that ATRA-mediated apoptotic cell death in neuroblastoma cells may be regulated in a p53-independent manner.

Differential expression of antiapoptotic Bcl-2 in neuroblastoma cells

To investigate the regulatory mechanisms of apoptotic response to ATRA in neuroblastoma cells, we examined the expression levels of Bcl-2 family proteins, which directly control the mitochondrial pathway of apoptosis. It is worth noting that antiapoptotic Bcl-2 was constitutively expressed at high levels in LA-N-5 as well as RTBM1 cells, whereas CHP134 and NB-39-nu cells expressed Bcl-2 at extremely low levels (Figure 3a). Antiapoptotic Bcl-x_L was expressed at low levels in all cell lines examined. In accordance with the previous observations showing that proapoptotic Bim and Bmf are highly expressed in neuronal cells (Puthalakath *et al*., 2001; Okuno *et al*., 2004; Shi *et al*., 2004), Bim and Bmf were expressed at high levels in all of the cell lines that we examined, but their expression levels remained unchanged in the presence of ATRA.

To determine whether Bcl-2 could contribute to the acquisition of the ATRA-resistant phenotype of neuroblastoma cells, CHP134 cells were transfected with the expression plasmid for Bcl-2 or with the empty plasmid, and their sensitivity to ATRA was examined by flow cytometry. As shown in Figure 3b, Bcl-2 was successfully overexpressed in CHP134 cells as examined by immunoblotting. Interestingly, enforced expression of Bcl-2 inhibited the ATRA-mediated proteolytic cleavage of caspase-3. Consistent with these results, flow cytometric analysis demonstrated that ectopic expression of Bcl-2 significantly reduced the number of cells with sub-G1 DNA content induced by ATRA treatment (Figure 3c and d), suggesting that Bcl-2 might play a critical role in the regulation of apoptotic cell death in neuroblastoma cells.

To further confirm this possibility, we examined the effects of the Bcl-2 inhibitor HA14-1 (Wang *et al*., 2000) on the ATRA-mediated apoptotic response of neuroblastoma cells. RTBM1 cells were treated with 5 μM of ATRA or left untreated for 6 days, and then incubated in the presence or absence of HA14-1 (15, 30 or 50 μM) for 3 h. Phase-contrast microscopic analysis showed that the incubation with ATRA followed by HA14-1 treatment significantly enhanced the apoptotic response of RTBM1 cells, whereas HA14-1 treatment alone increased the number of apoptotic cells to a lesser degree (Figure 4a). Similar results were also obtained by flow cytometric analysis (Figure 4b and c). To examine whether the ATRA-mediated apoptosis in RTBM1 cells induced by HA14-1 treatment could be associated with the activation of the mitochondria-dependent apoptotic pathway, we performed immunoblot analysis. As shown in Figure 4d, HA14-1 treatment at 30 μM or less did not promote the activation of caspase-9 and caspase-3, whereas a small amount of the cleaved caspase-9 and caspase-3 were detectable in RTBM1 cells exposed to 50 μM of HA14-1 alone. Intriguingly, pre-treatment of RTBM1 cells with ATRA enhanced the proteolytic cleavage of caspase-9 and caspase-3 induced by HA14-1 at a final concentration of 50 μM.

To ask whether Bcl-2 could play an important role in ATRA-mediated apoptotic response in primary neuroblastomas, 10 sporadically found neuroblastomas were subjected to both primary culture and reverse transcriptase–polymerase chain reaction (RT-PCR) analysis for *bcl-2*. In five cases, ATRA treatment induced strong outgrowth of neurites as compared with control culture (Figure 5a, left). In the other three cases, ATRA had undetectable effects (data not shown). It is worth noting that many cells underwent cell death after ATRA treatment in the remaining two cases (Figure 5a, right). We also examined the expression levels of *bcl-2* of these 10 primary neuroblastoma samples and four neuroblastoma-derived cell lines by RT–PCR. LA-N-5 and RTBM1 cells abundantly expressed *bcl-2*, whereas CHP134 and NB-39-nu did not (Figure 5b), which was consistent with immunoblotting as shown in Figure 3a. Of particular interest, RT–PCR analysis revealed that two primary cases that underwent cell death in response to ATRA (N-9 and N-10) expressed *bcl-2* at undetectable levels (Figure 5c). In a sharp contrast, the expression of *bcl-2* was detected in the remaining cases, except N-3. Taken together, our present results strongly suggest that Bcl-2 is a key regulator for ATRA-mediated apoptotic cell death in neuroblastoma cells.

Discussion

Retinoic acid is one of the potent antitumor agents that has been used successfully to treat certain human tumors including neuroblastomas (Freemantle *et al*., 2003). Indeed, neuroblastoma patients treated with RA have increased survival rate without severe side effects (Villablanca *et al*., 1995; Matthay *et al*., 1999). Accumulating evidences suggest that RA plays an important role in the regulation of neuroblastoma apoptosis as well as differentiation (Melino *et al*.,

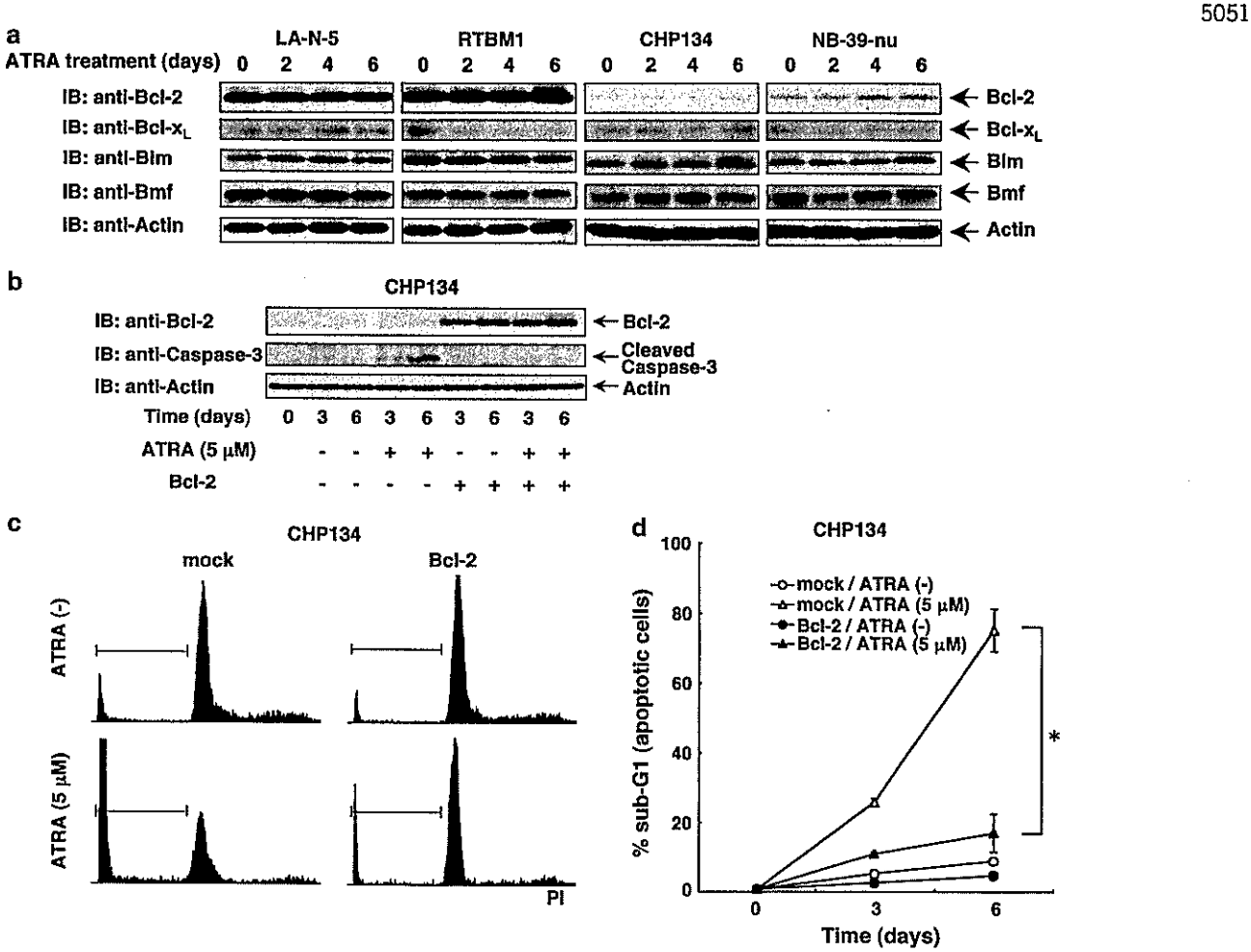

Figure 3 Differential expression of antiapoptotic Bcl-2 protein. (a) The indicated neuroblastoma cell lines were cultured in standard culture medium containing all-*trans* retinoic acid (ATRA) at a final concentration of 5 μM. At the indicated time points after the treatment with ATRA, whole-cell lysates were prepared, and analysed by immunoblotting with the antibodies against the indicated Bcl-2 family proteins. Actin expression was examined as a loading control (bottom). (b) Overexpression of Bcl-2. CHP134 cells were transiently transfected with the expression plasmid for Bcl-2 or with the empty plasmid. Twelve hours after the transfection, cells were treated with or without 5 μM ATRA, and incubated for additional 3 or 6 days. Whole-cell lysates were prepared, and the expression levels of Bcl-2 (top) and the amounts of the cleaved caspase-3 (middle) were examined by immunoblotting. Actin is shown as a control for protein loading (bottom). (c and d) Flow cytometry. CHP134 cells were transiently transfected as described in (b). At the indicated time periods after the treatment with ATRA, cells were collected, fixed and stained with PI. The DNA content of the cells was examined by flow cytometry. Representative results on day 6 are shown in (c). The number of cells with sub-G1 DNA content was counted in triplicate (d). $^*P<0.01$.

1997; van Noesel and Versteeg, 2004). However, certain neuroblastomas display an RA-resistant phenotype (Reynolds and Lemons, 2001). To further improve the therapeutic effects of RA on neuroblastomas, it is necessary to clarify the detailed molecular mechanisms underlying the RA-mediated neuroblastoma differentiation and/or apoptosis. In the present study, we have found that ATRA causes growth suppression and subsequent neuronal differentiation in human neuroblastoma-derived LA-N-5, RTBM1, CHP134 and NB-39-nu cells to various degrees. Among them, CHP134 and NB-39-nu cells, which express antiapoptotic Bcl-2 at extremely low levels, underwent p53-independent apoptotic cell death in response to ATRA. In contrast, LA-N-5 and RTBM1 cells abundantly expressed Bcl-2, and we did not detect apoptotic cell death upon ATRA treatment. Enforced expression of Bcl-2 in CHP134 cells inhibited the ATRA-mediated apoptosis, and HA14-1-mediated inhibition of the endogenous Bcl-2 in RTBM1 cells enhanced the ATRA-dependent apoptotic cell death. Moreover, studies using primary neuroblastoma tissues showed that ATRA had toxic effect on two out of 10 primary cultures, and these ATRA-sensitive tumors did not express *bcl-2*. Thus, it is likely that antiapoptotic Bcl-2 plays a crucial role in the regulation of the ATRA-mediated apoptotic response in neuroblastomas.

Our present study revealed that neuroblastoma cells can be divided into two groups with respect to the ATRA-induced apoptotic response. CHP134 and NB-39-nu cells underwent apoptotic cell death in response to ATRA, whereas LA-N-5 and RTBM1 cells did not. Consistent with the mitochondria-dependent intrinsic apoptotic pathway of caspase activation (Degterev

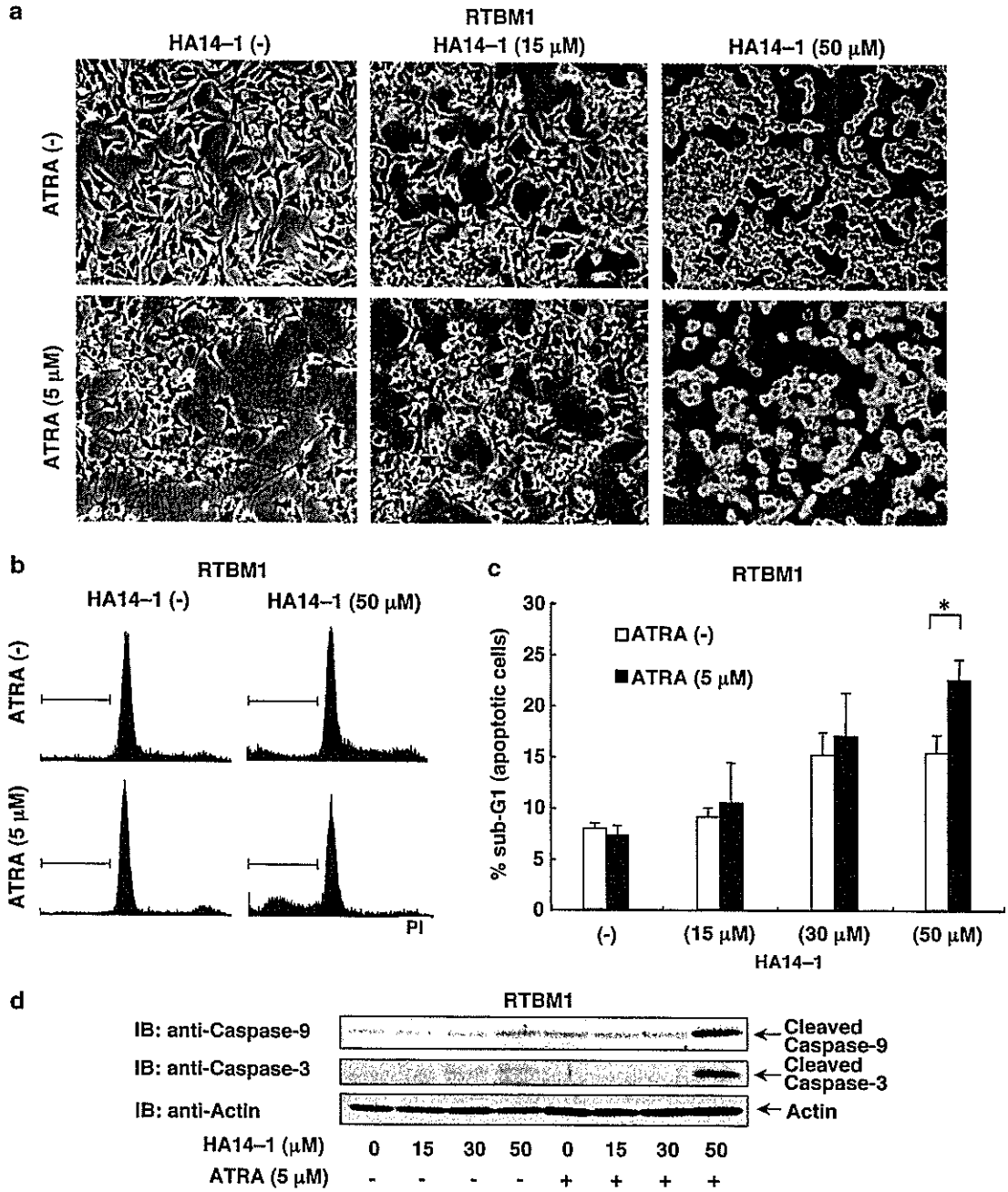

Figure 4 Bcl-2 inhibitor HA14-1 induces apoptosis of all-*trans* retinoic acid (ATRA)-treated RTBM1 cells. (a) Morphological changes after HA14-1 treatment of RTBM1 cells. RTBM1 cells were cultured with or without 5 μM ATRA for 6 days in advance, and then treated with HA14-1, a specific inhibitor of Bcl-2, at the indicated concentrations in standard medium for 3 h. Cells were examined by phase-contrast microscopy and photographed after the treatment. (b and c) FACS analysis. RTBM1 cells were treated with ATRA and HA14-1 as described in (a). Cells were collected, fixed and stained with PI. The DNA content of the cells was examined by flow cytometry and representative results are shown in (b). The number of cells with sub-G1 DNA content was counted in triplicate (c). $^*P<0.05$. (d) Immunoblotting. Whole-cell lysates of RTBM1 treated with ATRA and HA14-1 were prepared to examine the amounts of cleaved caspase-9 and caspase-3. Actin is shown as a loading control.

et al., 2003), ATRA treatment in CHP134 cells caused a cytoplasmic release of the mitochondrial inter-membrane protein cytochrome *c*, and a sequential proteolytic cleavage of caspase-9, caspase-3 and its physiological substrate PARP. Similar results were obtained in NB-39-nu cells. Our previous observation also demonstrated that activation and nuclear translocation of caspases were associated with prognosis of primary neuroblastomas (Nakagawara *et al.*, 1997). Therefore, the molecular mechanism(s) of RA-induced activation of caspases in neuroblastoma cells needs to be clarified.

In response to a variety of apoptotic stimuli, p53 is induced to be stabilized and subsequently transactivates a number of proapoptotic genes that encode Bcl-2

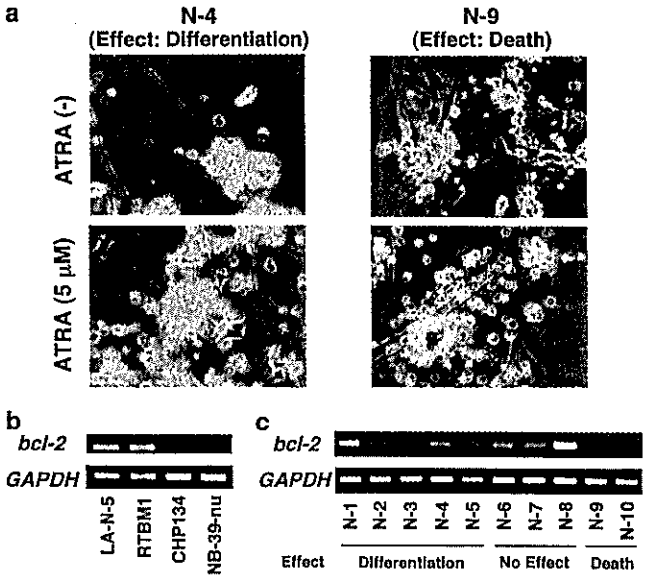

Figure 5 Primary culture and *bcl-2* expression of sporadic neuroblastomas. (a) Primary tumor cells prepared from 10 sporadically found neuroblastoma tissues were cultured with or without 5 μM of ATRA. After 4 days, cells were examined by phase-contrast microscope, and morphological changes of two representative cases are shown. (b and c) RT–PCR analysis. Total RNA was purified from the indicated neuroblastoma cell lines (b) and fresh-frozen tissues of primary neuroblastomas (c), and subjected to RT–PCR using specific primers for *bcl-2*. N-1 to N-10 indicates the case numbers, and the effects of ATRA on primary cultures are described at the bottom of this panel. Glyceraldehyde-3-phosphate dehydrogenase (*GAPDH*) expression is shown as an internal control.

family proteins including Bax (Culmsee and Mattson, 2005). It has been well documented that Bax acts on the mitochondria to induce mitochondrial permeability transition, and thereby regulating the cytoplasmic release of cytochrome *c* (Antonsson, 2001). Neuroblastoma cell lines that we examined in this study carry wild-type p53. Under our experimental conditions, however, we could not detect the ATRA-mediated upregulation of the endogenous p53 as well as Bax. Similarly, the p53-responsible $p21^{WAF1}$ and proapoptotic Puma were not accumulated in response to ATRA. As described (Nikolaev *et al.*, 2003), p53 might not be functional in neuroblastoma cells due to its abnormal cytoplasmic retention. Consistent with this notion, p53 was predominantly expressed in the cytoplasm of neuroblastoma cells examined in this study (data not shown). We have previously shown that cytoplasmic p53 is translocated into the nucleus of CHP134 cells in response to ATRA (Takada *et al.*, 2001); however, our present results suggest that translocated p53 was not functional. Indeed, it is reported that p53 in neuroblastoma cells is not functional even after its enforced translocation into the nucleus (Ostermeyer *et al.*, 1996). Thus, it is likely that the ATRA-mediated apoptotic cell death in neuroblastoma cells is regulated in a p53-independent manner.

Among other regulators of mitochondrial pathway of apoptosis, Bcl-2 family proteins are critical determinants of mitochondrial membrane potential, which controls the cytoplasmic release of cytochrome *c* from mitochondria and thereby regulating apoptotic cell death (Cory *et al.*, 2003). They are divided into two subfamilies based on their biological roles. Antiapoptotic subfamily includes Bcl-2 and Bcl-x_L and proapoptotic subfamily includes Bax, Bim and Bmf. The balance between these two groups determines the fate of cells. Antiapoptotic Bcl-2 is one of the most important members that inhibits the mitochondria-dependent apoptotic pathway triggered by diverse cytotoxic agents through blocking mitochondrial permeability transition. Indeed, the upregulation of Bcl-2 was associated with the drug-resistant phenotype of certain human tumors (Dole *et al.*, 1994; Lombet *et al.*, 2001). Most intriguingly, our expression studies revealed that antiapoptotic Bcl-2 was constitutively overexpressed in LA-N-5 and RTBM1 cells, whereas its expression levels were extremely low in CHP134 and NB-39-nu cells. In response to ATRA, Bcl-2 was slightly induced to be accumulated in NB-39-nu cells; however, it was maintained at extremely low levels in CHP134 cells. Furthermore, two primary neuroblastomas on which ATRA had toxic effect in primary culture did not express *bcl-2*, similar to CHP134 and NB-39-nu cells. Interestingly, ATRA induced differentiation in five cases and had undetectable effects on three cases, but cell death was induced in two cases. Considering that RA treatment contributed to survival of 17% of patients with aggressive neuroblastomas (Matthay *et al.*, 1999), our present results using primary neuroblastomas seem to be reliable. Taken together, it is likely that ATRA potentially have toxic effect on certain neuroblastoma cells (both primary cells and cell lines) that express little Bcl-2. Our current results also revealed that enforced expression of Bcl-2 in CHP134 cells inhibited the ATRA-mediated apoptosis in association with the activation of caspase-3. Furthermore, ATRA treatment of RTBM1 cells followed by HA14-1 exposure underwent apoptotic cell death through mitochondrial pathway. These observations also support the importance of Bcl-2 in the regulation of apoptotic response of neuroblastoma cells to RA.

Although it is still unclear whether the expression levels of Bcl-2 could be correlated with the prognosis of neuroblastoma patients (Romani and Lu, 1994; Gallo *et al.*, 2003; Abel *et al.*, 2005), it is possible that Bcl-2 plays a key role at least in part in the regulation of ATRA-mediated apoptotic cell death in neuroblastoma cells. In this connection, the antisense RNA-mediated knockdown of the endogeneous Bcl-2 has been employed to treat certain tumors (Kim *et al.*, 2004). Recently, a novel Bcl-2 inhibitor that has an antitumor effect on solid tumors has been developed (Oltersdorf *et al.*, 2005). Based on our present findings, the combination of RA with Bcl-2-specific inhibitor might provide a novel therapeutic strategy for the treatment of neuroblastomas, instead of the classical chemotherapy that frequently has multi-organ side effects.

Materials and methods

Cell lines and transfection

Human neuroblastoma-derived cell lines, including LA-N-5, RTBM1, CHP134 and NB-39-nu, were maintained in RPMI 1640 medium supplemented with 10% heat-inactivated fetal bovine serum, penicillin (50 U/ml) and streptomycin (50 μg/ml) at 37°C in a humidified atmosphere of 5% CO_2 in the air. For transfection, CHP134 cells were transfected with the expression plasmid encoding human Bcl-2 or with the empty plasmid by electroporation using a Nucleofector (Amaxa Biosystems, Koeln, Germany) according to the manufacturer's protocol.

Reagents

All-*trans* retinoic acid was purchased from Sigma (St Louis, MO, USA) dissolved in dimethylsulfoxisde (DMSO) at a final concentration of 5 mM, and kept at −80°C. Bcl-2 inhibitor HA14-1 was purchased from Sigma, dissolved in DMSO as a 10 mM stock solution and stored at −20°C. All reagents were of the highest quality available.

Proliferation assay

LA-N-5 and RTBM1 cells were plated in triplicate at a density of 1×10^5 per well in 12-well culture plates. CHP134 and NB-39-nu cells were seeded in triplicate at a density of 1×10^4 in 12-well plates. Twelve hours after seeding the cells, cells were treated with ATRA at a final concentration of 5 μM or left untreated, and medium was replaced every 2 days. At the indicated time points after the treatment with ATRA, cells were trypsinized and number of viable cells was directly scored by using the hemocytometer.

Flow cytometric analysis

Cells were exposed to the indicated concentration of ATRA. At the indicated time points after the treatment with ATRA, cells were collected by brief centrifugation, and fixed with 70% ethanol at −20°C. The cells were washed with phosphate-buffered saline (PBS), resuspended in phosphate-citrate buffer (4 mM citric acid, 200 mM Na_2HPO_4) and kept at room temperature for 15 min. The cells were then centrifuged and resuspended in a solution containing 40 μg/ml of propidium iodide and 0.05% RNase A, and incubated in the dark for 30 min. Before performing flow cytometric analysis, cells were filtered through a 40-μm nylon mesh. DNA content was analysed by FACScan flow cytometer (Becton Dickinson, Oxford, UK).

Immunoblot analysis

Cells were washed twice with ice-cold PBS, lysed in a sodium dodecyl sulfate (SDS)-sample buffer containing 10% glycerol, 5% β-mercaptoethanol, 2.3% SDS and 62.5 mM Tris-HCl, pH 6.8, and then boiled for 3 min. The protein concentrations were determined using Bio-Rad protein assay dye reagent (Bio-Rad Laboratories, Hercules, CA, USA). Bovine serum albumin (BSA) was used as a standard. Aliquots (20 μg) of whole-cell lysates were separated by SDS–polyacrylamide gel electrophoresis and electrophoretically transferred onto polyvinylidene difluoride membranes (Immobilon-P, Millipore, Bedford, MA, USA). The membranes were blocked with 0.3% non-fat milk in Tris-buffered saline containing 0.1% Tween-20 and incubated with appropriate primary antibodies at room temperature for 1 h followed by incubation with the horseradish peroxidase-conjugated secondary antibodies (Cell Signaling Technology Inc., Beverly, MA, USA). Immunoreactive bands were visualized by using ECL system (Amersham Biosciences, Uppsala, Sweden). The primary antibodies used in this study were as follows: polyclonal anti-caspase-12 (Cell Signalling Technology Inc.), polyclonal anti-caspase-3 (Calbiochem, San Diego, CA, USA), polyclonal anti-PARP (Cell Signaling Technology Inc.), polyclonal anti-PUMA (ab9643; Abcam, Cambridge, UK), polyclonal anti-$p21^{WAF1}$ (H-164; Santa Cruz Biotechnology), polyclonal anti-Bim (Cell Signaling Technology Inc.), polyclonal anti-Bmf (Cell Signaling Technology Inc.), polyclonal anti-actin (20-33; Sigma), monoclonal anti-caspase-8 (5F7; Medical & Biological Laboratories, Nagoya, Japan), monoclonal anti-caspase-9 (5B4; Medical & Biological Laboratories), monoclonal anti-p53 (DO-1; Oncogene Research Products, Cambridge, MA, USA), monoclonal anti-Bax (6A7; eBioscience, San Diego, CA, USA), monoclonal anti-Bcl-2 (100; Santa Cruz Biotechnology); and monoclonal anti-Bcl-x_L (H-5; Santa Cruz Biotechnology) antibodies.

Immunofluorescent staining

CHP134 cells were grown on coverslips in standard culture medium in the presence or absence of 5 μM of ATRA for 4 days. Cells were washed with ice-cold PBS, fixed with 3.7% formaldehyde in PBS for 30 min, permeabilized with 0.2% Triton X-100 in PBS for 5 min and then blocked with 3% BSA in PBS for 1 h at room temperature. After blocking, cells were incubated with a monoclonal antibody against cytochrome *c* (6H2.B4; BD PharMingen, San Jose, CA, USA) or with a normal mouse IgG for 1 h at room temperature, followed by the incubation with fluorescein isothiocyanate-conjugated secondary antibody against mouse IgG (Santa Cruz Biotechnology). The cell nuclei were stained with DAPI. The coverslips were mounted onto glass slides, and the stained cells were examined by using a confocal laser scanning microscope (Olympus).

Primary culture

RPMI 1640 medium supplemented with 10% heat-inactivated fetal bovine serum, penicillin (50 U/ml), streptomycin (50 μg/ml) and 100 μg/ml of OPI (Sigma) was used as a standard medium for primary culture. Primary tumor cells were prepared from fresh human neuroblastoma tissues by a standard method. A total of 5×10^5 cells of each sample were resuspended in 1 ml of the standard medium, and seeded on 24-well tissue culture plates precoated with collagen. The cells were treated with or without ATRA at a final concentration of 5 μM for at least 2 weeks. The effects of ATRA on the growth and neurite extension of primary neuroblastoma cells were examined by phase-contrast microscope.

RNA extraction and RT–PCR

Total RNA was prepared from fresh-frozen tissues of primary neuroblastomas or cultured cells by using RNeasy Mini Kit (Qiagen, Valencia, CA, USA). Total RNA (2 μg) was reverse transcribed by using random primers and SuperScript II reverse transcriptase (Invitrogen, Carlsbad, CA, USA). The resultant cDNA was subjected to PCR-based amplification. The oligonucleotide primers used in this study were as follows: *bcl-2*, 5′-GAGGATTGTGGCCTTCTTTG-3′ (forward) and 5′-ACAGTTCCACAAAGGCATCC-3′ (reverse), and glyceraldehyde-3-phosphate dehydrogenase (*GAPDH*), 5′-ACCTGACCTGCCGTCTAGAA-3′ (forward) and 5′-TCCACCACCCTGTTGCTGTA-3′ (reverse). PCR products were electrophoretically separated on 1% neutral agarose gels and visualized by ethidium bromide staining.

Acknowledgements

We are grateful to the hospitals and institutions that provided us with surgical specimens. We thank Hideki Yamamoto and Atsushi Kawasaki for valuable discussions, and Yuki Nakamura for excellent technical assistance. This work was supported in part by a Grant-in-Aid from the Ministry of Health, Labour and Welfare for Third Term Comprehensive Control Research for Cancer, and a Grant-in-Aid for Scientific Research on Priority Areas and a Grant-in-Aid for Scientific Research (C) from the Ministry of Education, Culture, Sports, Science and Technology, Japan.

References

Abel F, Sjoberg RM, Nilsson S, Kogner P, Martinsson T. (2005). *Eur J Cancer* **41**: 635–646.
Antonsson B. (2001). *Cell Tissue Res* **306**: 347–361.
Balmer JE, Blomhoff R. (2002). *J Lipid Res* **43**: 1773–1808.
Brodeur GM. (2003). *Nat Rev Cancer* **3**: 203–216.
Brodeur GM, Nakagawara A. (1992). *Am J Pediatr Hematol Oncol* **14**: 111–116.
Cory S, Huang DC, Adams JM. (2003). *Oncogene* **22**: 8590–8607.
Culmsee C, Mattson MP. (2005). *Biochem Biophys Res Commun* **331**: 761–777.
Degterev A, Boyce M, Yuan J. (2003). *Oncogene* **22**: 8543–8567.
Dole M, Nunez G, Merchant AK, Maybaum J, Rode CK, Bloch CA *et al.* (1994). *Cancer Res* **54**: 3253–3259.
Encinas M, Iglesias M, Llecha N, Comella JX. (1999). *J Neurochem* **73**: 1409–1421.
Freemantle SJ, Spinella MJ, Dmitrovsky E. (2003). *Oncogene* **22**: 7305–7315.
Gallo G, Giarnieri E, Bosco S, Cappelli C, Alderisio M, Giovagnoli MR *et al.* (2003). *Anticancer Res* **23**: 777–784.
Kim R, Emi M, Tanabe K, Toge T. (2004). *Cancer* **101**: 2491–2502.
Lee MH, Nikolic M, Baptista CA, Lai E, Tsai LH, Massague J. (1996). *Proc Natl Acad Sci USA* **93**: 3259–3263.
Lippman SM, Lotan R. (2000). *J Nutr* **130**: 479S–482S.
Lombet A, Zujovic V, Kandouz M, Billardon C, Carvajal-Gonzalez S, Gompel A *et al.* (2001). *Eur J Biochem* **268**: 1352–1362.
Lopez-Carballo G, Moreno L, Masia S, Perez P, Barettino D. (2002). *J Biol Chem* **277**: 25297–25304.
Maden M. (2001). *Int Rev Cytol* **209**: 1–77.
Matthay KK, Villablanca JG, Seeger RC, Stram DO, Harris RE, Ramsay NK *et al.* (1999). *N Engl J Med* **341**: 1165–1173.
McCaffery PJ, Adams J, Maden M, Rosa-Molinar E. (2003). *Eur J Neurosci* **18**: 457–472.
Melino G, Thiele CJ, Knight RA, Piacentini M. (1997). *J Neurooncol* **31**: 65–83.
Morishima N, Nakanishi K, Takenouchi H, Shibata T, Yasuhiko Y. (2002). *J Biol Chem* **277**: 34287–34294.
Nagai J, Yazawa T, Okudela K, Kigasawa H, Kitamura H, Osaka H. (2004). *Cancer Res* **64**: 7910–7917.
Nakagawa T, Zhu H, Morishima N, Li E, Xu J, Yankner BA *et al.* (2000). *Nature* **403**: 98–103.
Nakagawara A. (1998). *Hum Cell* **11**: 115–124.
Nakagawara A, Arima-Nakagawara M, Scavarda NJ, Azar CG, Cantor AB, Brodeur GM. (1993). *N Engl J Med* **328**: 847–854.
Nakagawara A, Azar CG, Scavarda NJ, Brodeur GM. (1994). *Mol Cell Biol* **14**: 759–767.
Nakagawara A, Nakamura Y, Ikeda H, Hiwasa T, Kuida K, Su MS *et al.* (1997). *Cancer Res* **57**: 4578–4584.
Nakamura Y, Ozaki T, Koseki H, Nakagawara A, Sakiyama S. (2003). *Biochem Biophys Res Commun* **307**: 206–213.
Nikolaev AY, Li M, Puskas N, Qin J, Gu W. (2003). *Cell* **112**: 29–40.
Okuno S, Saito A, Hayashi T, Chan PH. (2004). *J Neurosci* **24**: 7879–7887.
Oltersdorf T, Elmore SW, Shoemaker AR, Armstrong RC, Augeri DJ, Belli BA *et al.* (2005). *Nature* **435**: 677–681.
Ostermeyer AG, Runko E, Winkfield B, Ahn B, Moll UM. (1996). *Proc Natl Acad Sci USA* **93**: 15190–15194.
Piacentini M, Annicchiarico-Petruzzelli M, Oliverio S, Piredda L, Biedler JL, Melino G. (1992). *Int J Cancer* **52**: 271–278.
Puthalakath H, Villunger A, O'Reilly LA, Beaumont JG, Coultas L, Cheney RE *et al.* (2001). *Science* **293**: 1829–1832.
Reynolds CP, Lemons RS. (2001). *Hematol Oncol Clin N Am* **15**: 867–910.
Romani P, Lu QL. (1994). *J Pathol* **172**: 273–278.
Schor NF. (1999). *J Neurooncol* **41**: 159–166.
Shi L, Gong S, Yuan Z, Ma C, Liu Y, Wang C *et al.* (2004). *Neurosci Lett* **375**: 7–12.
Takada N, Isogai E, Kawamoto T, Nakanishi H, Todo S, Nakagawara A. (2001). *Med Pediatr Oncol* **36**: 122–126.
Teitz T, Wei T, Valentine MB, Vanin EF, Grenet J, Valentine VA *et al.* (2000). *Nat Med* **6**: 529–535.
Thiele CJ, Reynolds CP, Israel MA. (1985). *Nature* **313**: 404–406.
Van Noesel MM, Van Bezouw S, Voute PA, Herman JG, Pieters R, Versteeg R. (2003). *Genes Chromosomes Cancer* **38**: 226–233.
Van Noesel MM, Versteeg R. (2004). *Gene* **325**: 1–15.
Villablanca JG, Khan AA, Avramis VI, Seeger RC, Matthay KK, Ramsay NK *et al.* (1995). *J Clin Oncol* **13**: 894–901.
Wang JL, Liu D, Zhang ZJ, Shan S, Han X, Srinivasula SM *et al.* (2000). *Proc Natl Acad Sci USA* **97**: 7124–7129.

Oncogene (2006) 25, 7608–7617

www.nature.com/onc

ORIGINAL ARTICLE

NF-κB regulates the stability and activity of p73 by inducing its proteolytic degradation through a ubiquitin-dependent proteasome pathway

H Kikuchi[1,2,3], T Ozaki[1,3], K Furuya[1], T Hanamoto[1,2], M Nakanishi[1], H Yamamoto[1], K Yoshida[1], S Todo[2] and A Nakagawara[1]

[1]Division of Biochemistry, Chiba Cancer Center Research Institute, Chiba, Japan and [2]Department of General Surgery, Hokkaido University School of Medicine, Kita-ku, Sapporo, Japan

Nuclear factor kappa B (NF-κB), which exists as heterodimeric complexes composed of p50 and p65, has been shown to play an important role in cell survival processes. In the present study, we found for the first time that NF-κB has an ability to induce the ubiquitin-dependent proteasomal degradation of proapoptotic p73α. The activation of NF-κB in tumor necrosis factor α (TNF-α)-stimulated H1299 cells resulted in a significant reduction in the amounts of the endogenous p73α. Consistent with these results, TNF-α-mediated down-regulation of p73α was observed in wild-type (WT) mouse embryonic fibroblasts (MEFs) but not in p65-deficient MEFs. Ectopic expression of NF-κB decreased a half-life of p73α by increasing its ubiquitination levels, and thereby inhibiting the transcriptional activity as well as proapoptotic function of p73α, whereas NF-κB had undetectable effects on p53. Immunoprecipitation experiments demonstrated that, under our experimental conditions, NF-κB does not bind to p73α in mammalian cultured cells. In contrast to WT p65, the COOH-terminal deletion mutant of p65 (p65ΔC) failed to reduce the expression levels of p73α, suggesting that NF-κB-mediated proteolytic degradation of p73α requires the transcriptional activity of NF-κB. Taken together, our present results imply that NF-κB-mediated degradation of proapoptotic p73 is a novel inhibitory mechanism of p73 that regulates cell survival and death.

Oncogene (2006) **25**, 7608–7617. doi:10.1038/sj.onc.1209748; published online 4 September 2006

Keywords: apoptosis; NF-κB; p53; p73; ubiquitination

Introduction

p73 and p63 share a significant amino-acid sequence similarity to p53, and exist as multiple isoforms arising from alternative splicing termed the TA variants (Kaghad *et al.*, 1997; Yang *et al.*, 1998), or from alternative promoter usage termed the ΔN variants (Yang and McKeon, 2000; Melino *et al.*, 2002; Stiewe and Putzer, 2002). Recently, it has been shown that p53 is also expressed as multiple variants (Bourdon *et al.*, 2005). These TA variants function in a manner similar to p53 by inducing G1 cell cycle arrest or apoptosis in certain cancerous cells through transactivating an overlapping set of p53/p73-responsive downstream effectors such as $p21^{WAF1}$ and BAX (Jost *et al.*, 1997; Kaghad *et al.*, 1997; Gressner *et al.*, 2005). Among these TA variants of p73, p73α has an extended COOH-terminal region including SAM (sterile α motif) domain and the extreme COOH-terminus. In marked contrast to p53, p73 is rarely mutated in human tumors despite an extensive search (Ikawa *et al.*, 1999). The initial genetic studies demonstrated that p73-deficient mice exhibit neurological defects, but do not develop any spontaneous tumors (Yang *et al.*, 2000), suggesting that p73 does not function as a classical tumor suppressor. Intriguingly, Flores *et al.* (2002) found that the indirect contribution of p73 or p63 is required for the p53-dependent apoptosis. Thus, it is likely that p73 cooperates with p53 to induce apoptosis and/or exerts its proapoptotic activity in a p53-independent manner.

ΔNp73, which lacks the NH_2-terminal transactivation domain, has an oncogenic potential, and acts in a dominant-negative fashion toward wild-type (WT) p53 as well as p73 (Pozniak *et al.*, 2000; Yang *et al.*, 2000; Stiewe *et al.*, 2002). Pozniak *et al.* (2000) demonstrated that ΔNp73 is predominantly expressed in sympathetic neurons, and inhibits p53-dependent neuronal apoptosis. Of note, we and others found that p73 directly binds to the canonical p53/p73-responsive element within the ΔNp73 promoter region, and strongly upregulates the expression of its own negative regulator ΔNp73, indicating that there exists the negative feedback regulation of p73 by its transcriptional target ΔNp73 (Grob *et al.*, 2001; Nakagawa *et al.*, 2002; Zaika *et al.*, 2002).

p73 is kept at extremely low level in mammalian cells, keeping p73 in an inactive state. Previous studies revealed that p73 is induced to be accumulated in response to a wide variety of DNA-damaging agents (Irwin *et al.*, 2003). For example, cisplatin or ionizing radiation triggers phosphorylation of p73 at Tyr-99

Correspondence: Dr A Nakagawara, Division of Biochemistry, Chiba Cancer Center Research Institute, 666-2 Nitona, Chuoh-ku, Chiba 260-8717, Japan.
E-mail: akiranak@chiba-cc.jp
[3]These authors contributed equally to this work.
Received 7 February 2006; revised 28 April 2006; accepted 10 May 2006; published online 4 September 2006

mediated by nonreceptor tyrosine kinase c-Abl, increasing its stability at protein level and proapoptotic activity (Agami *et al.*, 1999; Gong *et al.*, 1999). Alternatively, it has been shown that the prolyl isomerase Pin1 as well as the transcriptional coactivator Yes-associated protein YAP enhances p73 acetylation mediated by p300 in response to DNA damage, and thereby increasing p73 stability (Mantovani *et al.*, 2004; Strano *et al.*, 2005). These observations suggest that the stress-induced chemical modifications of p73 play a critical role in regulating p73 stability and activity. Accumulating evidence strongly suggests that p73 protein level is regulated in a ubiquitin-mediated proteasomal degradation pathway (Balint *et al.*, 1999; Lee and La Thangue, 1999; Bernassola *et al.*, 2004). Unlike p53, MDM2 binds to the NH_2-terminal transactivation domain of p73 and inhibits its transcriptional activity but does not target p73 for ubiquitin-mediated degradation (Balint *et al.*, 1999; Zeng *et al.*, 1999), implying that the protein stability of p73 is regulated through a pathway distinct from that of p53.

The activation of nuclear factor κB (NF-κB) has been shown to play an important role in the control of cell survival processes, which protects cells from a wide variety of apoptotic stresses (Beg and Baltimore, 1996; Van Antwerp *et al.*, 1996; Wang *et al.*, 1996, 1998). For example, camptothecin-mediated activation of NF-κB provides an antiapoptotic function (Huang *et al.*, 2000), and inhibition of NF-κB results in radiosensitization (Yamagishi *et al.*, 1997). Tumor necrosis factor alpha (TNF-α) activates the NF-κB-mediated cellular protective mechanism against the proapoptotic effect of TNF-α through the induction of the NF-κB-target genes that are involved in the inhibition of apoptosis (Beg and Baltimore, 1996; Van Antwerp *et al.*, 1996; Wang *et al.*, 1996). In addition to the antiapoptotic effect of NF-κB, NF-κB also contributes to cellular transformation and oncogenesis. Consistent with this notion, constitutive high levels of NF-κB activity were detectable in various human tumors (Bayon *et al.*, 2003). Intriguingly, Wan and DeGregori (2003) reported that NF-κB promotes T-cell survival in response to antigenic stimulation through the downregulation of p73; however, the precise molecular mechanism behind the NF-κB-mediated reduction of p73 is less well understood.

In the present study, we have found for the first time that NF-κB activation promotes the ubiquitin-dependent proteasomal turnover of p73, and the transcriptional activity of NF-κB is required for the NF-κB-mediated degradation of p73. Our present findings provide an evidence that NF-κB-mediated degradation of p73 might be a novel inhibitory mechanism of p73 function.

Results

Ectopic expression of NF-κB decreases p73α level

We first asked whether NF-κB could affect the expression level of proapoptotic p73. To this end, p53-deficient H1299 cells were co-transfected with the constant amount of the expression plasmid for FLAG-p73α together with or without the increasing amounts of the HA-p65 plus HA-p50 expression plasmids. At 48 h after transfection, whole-cell lysates were prepared, and immunoblot analysis revealed that the expression level of FLAG-p73α is significantly reduced in cells co-expressing HA-p65 and HA-p50 in a dose-dependent manner (Figure 1a). Under our experimental conditions, *p73α* mRNA level remained unchanged even in the presence of the exogenous HA-p65 and HA-p50. Similar results were also obtained in COS7 cells (Figure 1b). Next, we examined the effect of ectopically expressed NF-κB on the endogenous p73. COS7 cells were co-transfected with or without the increasing amounts of the expression plasmids encoding HA-p65 plus HA-p50. At 48 h after transfection, whole-cell lysates were immunoprecipitated with the normal mouse serum (NMS) or with the anti-p73 antibody, followed by immunoblotting with the anti-p73 antibody. As shown in Figure 1c and d, the endogenous p73α was significantly decreased at protein level in the presence of the ectopically expressed HA-p65 and HA-p50.

NF-kB specifically downregulates p73α

We tested whether NF-κB could reduce the expression levels of the other p53 family members including p53 and p63. Figure 2a shows the domain structures of p53, p73α, p73β and p63α. Whole-cell lysates prepared from H1299 cells transiently co-transfected with the indicated combinations of the expression plasmids were analysed for the expression levels of FLAG-p53, FLAG-p73β and p63α. In a sharp contrast to p73α, the enforced expression of NF-κB had marginal effects on the levels of FLAG-p53, FLAG-p73β and p63α (Figure 2b–d). Under our experimental conditions, NF-κB had undetectable effect on ΔNp73 (data not shown). These results strongly suggest that NF-κB-mediated downregulation is highly specific to p73α.

TNF-α-mediated activation of NF-κB results in a downregulation of the endogenous p73α

We sought to examine whether the activation of the endogenous NF-κB could affect the expression level of the endogenous p73. H1299 cells stably transfected with the NF-κB luciferase reporter plasmid (Muta and Takeshige, 2001) were treated with TNF-α as indicated, and their luciferase activity was determined. As shown in Figure 3a–c, TNF-α treatment enhanced the NF-κB-dependent transcriptional activation, and p65 as well as p50 translocated into cell nucleus in response to TNF-α as examined by immunoblotting and indirect immunofluorescence staining. As expected, immunoprecipitation experiments demonstrated that the expression level of the endogenous p73α protein is significantly reduced in response to TNF-α, whereas *p73α* mRNA level remained unchanged in cells exposed to TNF-α (Figure 3d). TNF-α treatment had no significant effects on the viability of cells (data not shown). These results suggest that the TNF-α-mediated activation of NF-κB leads to a

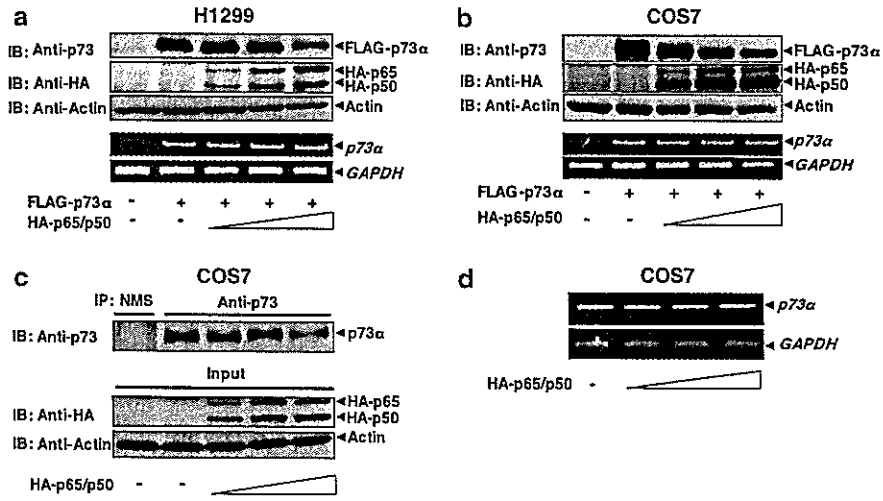

Figure 1 NF-κB decreases the amount of p73α. (a and b) Downregulation of p73α by NF-κB. H1299 (a) or COS7 (b) cells were co-transfected with the constant amount of the expression plasmid for FLAG-p73α (0.5 μg) together with or without the increasing amounts of the HA-p65 and HA-p50 expression plasmids (0.5, 1.0 and 1.5 μg). At 48 h after transfection, whole-cell lysates or total RNA were subjected to immunoblotting or RT–PCR analysis, respectively. Expression of FLAG-p73α, HA-p65 and HA-p50 was verified by the indicated antibodies. Actin was used to confirm that an equivalent amount of protein was loaded into each lane. For RT–PCR, ethidium bromide staining of *GAPDH* confirmed equivalent loading. (c and d) Downregulation of the endogenous p73α by the enforced expression of NF-κB. COS7 cells were co-transfected with or without the increasing amounts of HA-p65 and p50 expression plasmids. At 48 h after transfection, whole-cell lysates or total RNA were processed for the immunoprecipitation with the NMS or with the anti-p73 antibody, or subjected to RT–PCR, respectively.

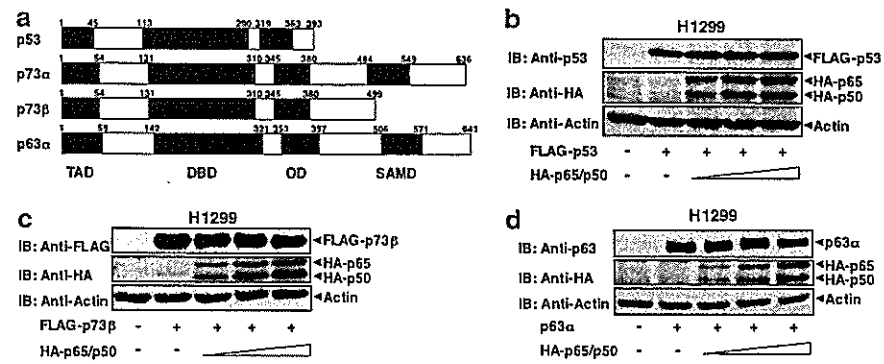

Figure 2 NF-κB-dependent downregulation is specific to p73α. (a) Domain structure of p53 family members. The transactivation domain (TAD), DNA-binding domain (DBD), oligomerization domain (OD), and SAM domain are indicated. (b–d) NF-κB does not affect the expression levels of p53, p73β and p63α. H1299 cells were co-transfected with the constant amount of the expression plasmid for FLAG-p53 (b), FLAG-p73β (c) or p63α (d) along with or without the increasing amounts of the expression plasmids for HA-p65 and HA-p50. At 48 h after transfection, whole-cell lysates were analysed by immunoblotting with the indicated antibodies. The *lower panels* show actin to demonstrate equal loading of the gels.

reduction in the amounts of proapoptotic p73α at protein level. In contrast to TNF-α, cisplatin treatment had negligible effects on the transcriptional activity of NF-κB, and immunoprecipitation experiments revealed that the endogenous p73α is induced to be accumulated in cells exposed to cisplatin (Supplementary Figure S1).

To confirm our hypothesis that the downregulation of p73α is dependent on NF-κB, we further investigated whether the expression level of the endogenous p73α could be altered in the absence of heterodimeric complex of NF-κB. To this end, we used mouse embryonic fibroblasts (MEFs) derived from p65 knockout mice (Figure 4a) (Beg *et al.*, 1995). Whole-cell lysates were prepared from p65 knockout and WT MEFs exposed to TNF-α (20 ng/ml) or left untreated. Immunoprecipitation experiments demonstrated that TNF-α-mediated reduction of the endogenous p73α is observed in WT MEFs but not in p65 knockout MEFs (Figure 4b and c), indicating that the presence of functional NF-κB complex is required for the downregulation of p73α.

NF-κB stimulates the ubiquitin-dependent proteasomal degradation of p73α

To determine whether NF-kB could modulate p73α turnover, we sought to examine the half-life of p73α in the presence or absence of the exogenously expressed NF-κB using cycloheximide blockade. COS7 cells were

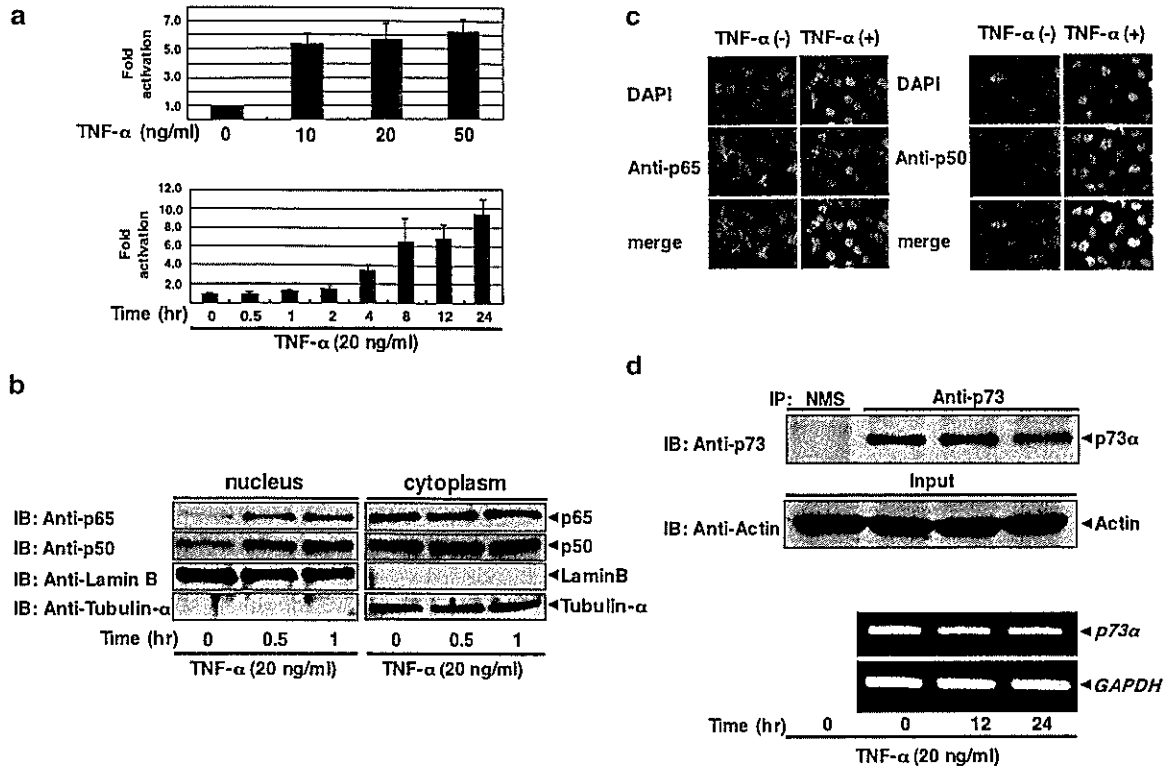

Figure 3 TNF-α treatment causes a downregulation of the endogenous p73α. (a) TNF-α treatment enhances the transcriptional activity of NF-κB. H1299 cells stably transfected with the luciferase reporter plasmid carrying 1xκB site and *Renilla* luciferase construct were exposed to the indicated concentrations of TNF-α for 24 h (upper panel) or treated with 20 ng/ml of TNF-α for the indicated time periods (lower panel). At the indicated time periods after the treatment with TNF-α, luciferase assays were performed. (b and c) Nuclear translocation of p65 and p50 in response to TNF-α. H1299 cells exposed to TNF-α (20 ng/ml) for the indicated time periods were separated into nuclear and cytoplasmic fractions. The aliquots of these fractions were analysed by immunoblotting with the anti-p65 (1st panel) or with the anti-p50 (2nd panel) antibody. These fractions were also analysed for nucleus-specific Lamin B (3rd panel) and cytoplasm-specific α-tubulin (4th panel) to show the validity of our fractionation technique (b). H1299 cells were treated with TNF-α (20 ng/ml) for 1 h or left untreated. Cells were fixed and then incubated with the anti-p65 (left panels) or with the anti-p50 (right panels) antibody. Cell nuclei were stained by DAPI. Cellular localization was detected by fluorescence microscopy. The merged images indicate the nuclear translocation of p65 and p50 in response to TNF-α (c). (d) TNF-α treatment decreases the expression level of the endogenous p73α. H1299 cells were treated with TNF-α (20 ng/ml) for the indicated time periods or left untreated. Whole-cell lysates or total RNA were subjected to immunoprecipitation with the indicated antibodies or RT–PCR, respectively.

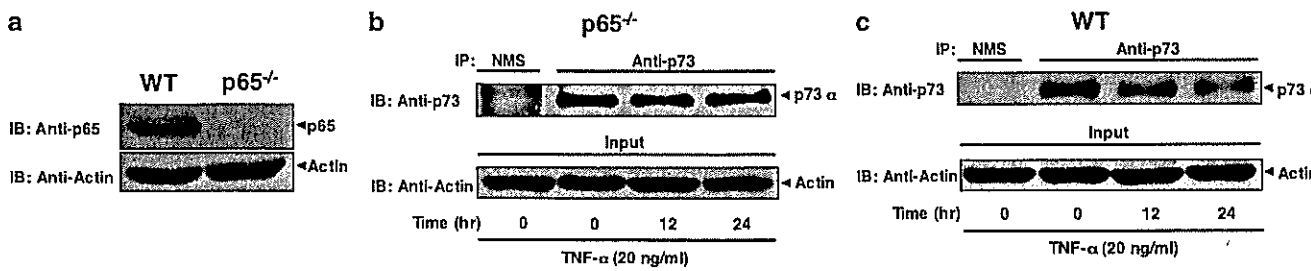

Figure 4 NF-κB-dependent reduction of p73 in response to TNF-α. (a) Expression of the endogenous p65 in MEFs. Whole-cell lysates from WT and p65 knockout MEFs were analysed for p65 by immunoblotting. (b and c) TNF-α-dependent downregulation of the endogenous p73α is observed in WT but not in p65 knockout MEFs. p65 knockout (b) and WT (c) MEFs were treated with TNF-α (20 ng/ml) for indicated time periods or left untreated. Whole-cell lysates were subjected to immunoprecipitation with NMS or with the anti-p73 antibody, followed by immunoblotting with the anti-p73 antibody.

co-transfected with the constant amount of the expression plasmid for FLAG-p73α along with or without the constant amount of the expression plasmids encoding HA-p65 and HA-p50. At 24 h after transfection, cells were exposed to cycloheximide (100 μg/ml). At the indicated time points, whole-cell lysates were subjected to immunoblotting with the anti-p73 antibody. Consistent with the previous observations (Lee and La Thangue, 1999), transiently expressed FLAG-p73α had a half-life of about 3 h (Figure 5a). When FLAG-p73α was co-expressed with HA-p65 and HA-p50, the degradation rate of FLAG-p73α was faster than that

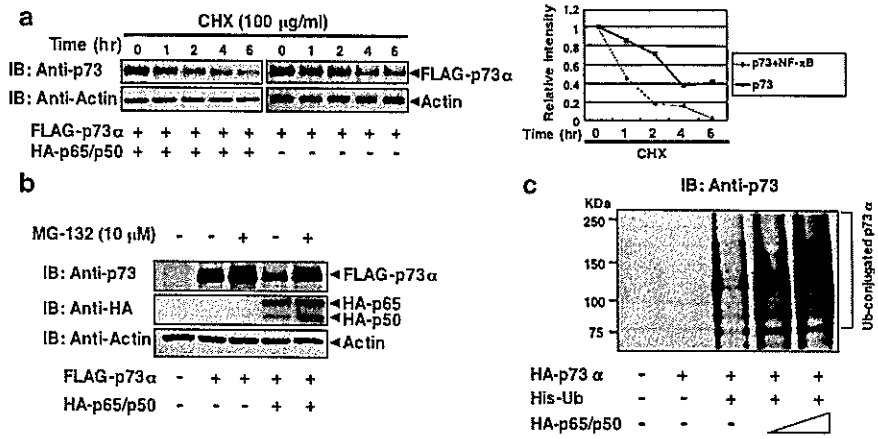

Figure 5 NF-κB-induced reduction of p73 is regulated by a ubiquitin–proteasome pathway. (a) NF-κB decreases a half-life of p73α. COS7 cells were co-transfected with the constant amount of the FLAG-p73α expression plasmid together with or without the expression plasmids for HA-p65 and HA-p50. At 24 h after transfection, cells were exposed to cycloheximide (100 μg/ml). At the indicated time points after the addition of cycloheximide, whole-cell lysates were analysed for FLAG-p73α by immunoblotting. Actin was used for equal protein loading. Densitometry was used to quantify the amounts of FLAG-p73α, which normalized to actin. (b) NF-κB-mediated degradation of p73α is blocked by proteasomal inhibitor. COS7 cells were transfected either with FLAG-p73α alone or with FLAG-p73α, HA-p65 and HA-p50. At 40 h after transfection, cells were treated with or without MG-132 (10 μM) for 6 h. Whole-cell lysates were subjected to immunoblotting with the anti-p73, anti-HA or with anti-actin antibody. (c) NF-κB increases the ubiquitination levels of p73. COS7 cells were co-transfected with the constant amount of the expression plasmids for HA-p73α and His-Ub together with or without the increasing amounts of the HA-p65 and HA-p50 expression plasmids. At 40 h post-transfection, cells were treated with MG-132 (10 μM) for 6 h. Whole-cell lysates were then prepared, and ubiquitinated materials were recovered by Ni^{2+}-NTA-agarose beads, followed by immunoblotting with the anti-p73 antibody.

in cells expressing FLAG-p73α alone (a half-life of about 1 h). In addition, NF-κB had undetectable effects on the half-life of ΔNp73 (data not shown).

According to the previous reports (Balint *et al*., 1999; Lee and La Thangue, 1999; Bernassola *et al*., 2004), p73 protein level is regulated through the ubiquitin-mediated proteasomal degradation pathway. We then determined the effects of proteasomal inhibitor MG-132 on the expression level of p73α. As expected, proteasome inhibition resulted in a stabilization of FLAG-p73α (Figure 5b). Of note, the addition of MG-132 blocked the NF-κB-mediated degradation of FLAG-p73α, indicating that NF-κB-mediated degradation of p73α is regulated at least in part through the proteasomal pathway. To ask whether NF-κB could affect the ubiquitination levels of p73α, COS7 cells were co-transfected with the constant amount of the HA-p73α expression plasmid and the expression plasmid for His-tagged ubiquitin together with or without the increasing amounts of the expression plasmids for HA-p65 and HA-p50. After the treatment with MG-132 for 6 h, whole-cell lysates were prepared, and the ubiquitinated materials were recovered with Ni^{2+}-agarose beads followed by immunoblotting with the anti-p73 antibody. As shown in Figure 5c, ubiquitin-conjugated p73α was significantly increased upon the co-expression of HA-p73α with HA-p65 and HA-p50. Thus, it is likely that NF-κB mediates the ubiquitin-dependent proteasomal turnover of p73α.

NF-κB inhibits the transcriptional activity of p73α but not of p53

To evaluate whether NF-κB could influence the transcriptional activity of p73α, H1299 cells were co-transfected with the constant amount of the expression plasmid for FLAG-p73α, and the luciferase reporter construct controlled by the p53/p73-responsive element from the *BAX* or *MDM2* promoter together with or without the increasing amounts of the expression plasmids for HA-p65 and HA-p50. At 48 h after transfection, the luciferase activities were measured. As shown in Figure 6a, co-expression of FLAG-p73α with HA-p65 and HA-p50 significantly reduced the p73α-mediated transcriptional activation of *BAX* and *MDM2* promoters in a dose-dependent manner, and HA-p65 and HA-p50 had negligible effects on the reporter gene activities. Consistent with these results, RT–PCR analysis revealed that enforced expression of HA-p65 and HA-p50 inhibits the p73α-mediated transactivation of the endogenous *BAX*. In contrast, p53-mediated transcriptional activation was not affected in cells co-transfected with the HA-p65 and HA-p50 expression plasmids (Figure 6b).

NF-κB inhibits the proapoptotic activity of p73α

To further confirm the inhibitory effects of NF-κB on the p73 function, we examined the possible effects of NF-κB on the proapoptotic activity of p73α. H1299 cells were co-transfected with the indicated combinations of the expression plasmids. At 48 h after the transfection, cells were fixed, stained with propidium iodide, and the numbers of cells with sub-G1 DNA content were measured. In accordance with the previous report (Jost *et al*., 1997), expression of FLAG-p73α resulted in an increase in number of cells with sub-G1 DNA content (Figure 6c). Co-expression of FLAG-p73α with HA-p65 and HA-p50 decreased number of cells with sub-G1 DNA content in a dose-dependent manner. Additionally,

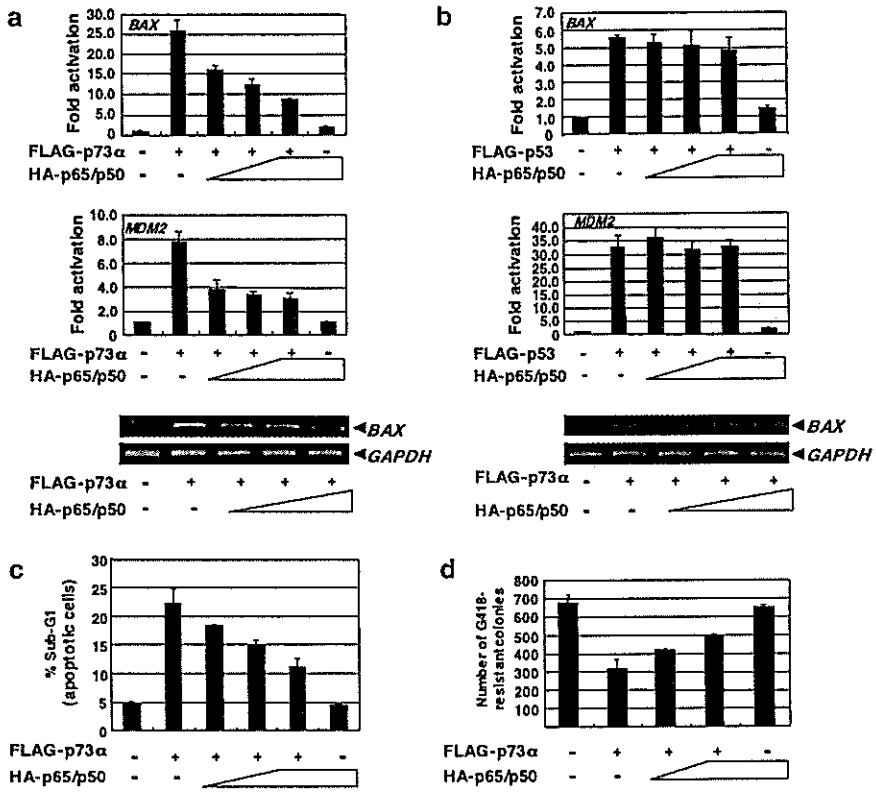

Figure 6 NF-κB inhibits the transcriptional as well as proapoptotic activity of p73. (a and b) NF-κB-mediated inhibition of the p73α-dependent transactivation but not of p53. H1299 cells were co-transfected with 25 ng of the expression plasmid for FLAG-p73α (a) or FLAG-p53 (b) together with 100 ng of the luciferase reporter construct, which carries the p53/p73-responsive element derived from *BAX* or *MDM2* promoter and 10 ng of the *Renilla* luciferase plasmid (pRL-TK) in the presence or absence of the increasing amounts of HA-p65 and HA-p50 expression plasmids (50, 100, or 200 ng). All transfections were performed in triplicate. At 48 h after transfection, cells were analysed for their luciferase activities. Firefly luminescence signal was normalized based on the *Renilla* luminescence signal. Results were shown as fold induction of the firefly luciferase activity compared with control cells transfected with the empty plasmid alone. For RT–PCR analysis, H1299 cells were co-transfected with the FLAG-p73α or FLAG-p53 expression plasmid together with or without the increasing amounts of the HA-p65 and HA-p50 expression plasmids. At 48 h post-transfection, total RNA was subjected to RT–PCR analysis for the expression of *BAX*. Amplification of *GAPDH* serves as an internal control. (c) FACS analysis. H1299 cells were co-transfected with the constant amount of the expression plasmid encoding FLAG-p73α together with or without the increasing amounts of the HA-p65 and HA-p50 expression plasmids. At 48 h after transfection, cells were fixed and stained with propidium iodide. (d) Colony formation assay. H1299 cells were co-transfected with the indicated combinations of the expression plasmids. At 24 h after transfection, cells were selected with G418 (400 μg/ml) for 2 weeks. The number of G418-resistant colonies was scored.

colony formation assays demonstrated that co-expression of FLAG-p73α with the increasing amounts of the HA-p65 and HA-p50 increases number of G418-resistant colonies as compared with that in cells expressing FLAG-p73α alone (Figure 6d). Taken together, these results strongly suggest that NF-κB has an ability to inhibit the transcriptional activity as well as proapoptotic function of p73α.

NF-κB does not bind to p73α in cells

To investigate how NF-κB decreases the stability and activity of p73α, we examined whether NF-κB could bind to p73α. H1299 cells were co-transfected with the indicated combinations of the expression plasmids. At 48 h after transfection, whole-cell lysates were immunoprecipitated with the anti-FLAG or anti-HA antibody followed by immunoblotting with the anti-HA or anti-p73 antibody, respectively. As shown in Figure 7a, the anti-FLAG immunoprecipitates did not contain HA-p65 and HA-p50. Similarly, FLAG-p73α was not co-immunoprecipitated with HA-p65 and HA-p50 (Figure 7b). Under our experimental conditions, FLAG-p73α was co-immunoprecipitated with MDM2 (data not shown), which was consistent with the previous reports (Balint *et al*., 1999; Zeng *et al*., 1999). Thus, it is likely that NF-κB-mediated inhibitory effects on p73α might be indirect without a direct interaction between them.

Transactivation function of NF-κB is required for the downregulation of p73α

To determine the molecular mechanism by which NF-κB contributes to the degradation of p73α, we focused on the COOH-terminal transactivation domain of p65 (Figure 7c). We generated a deletion mutant of p65 (HA-p65ΔC), which retains a nuclear localization signal but lacks a COOH-terminal transactivation domain. To assess the transactivation function of p65ΔC, we

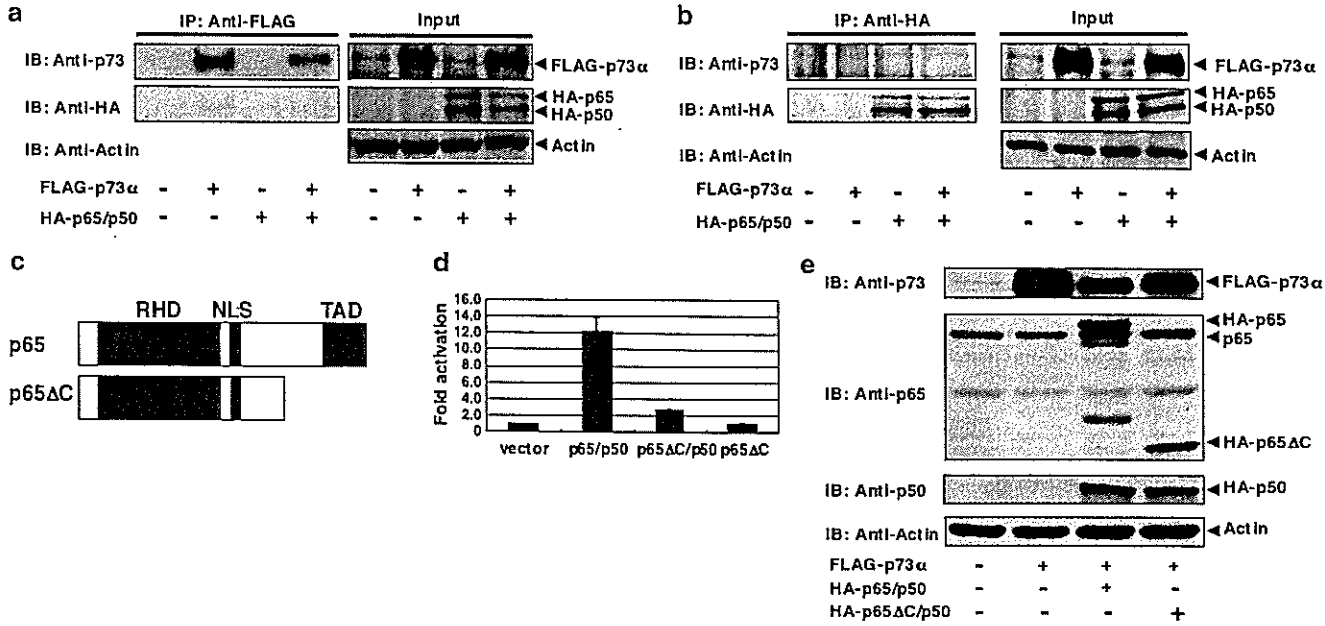

Figure 7 Transcriptional activity of NF-κB is required for the down regulation of p73. (a and b) Immunoprecipitation experiments. H1299 cells were co-transfected with the indicated combinations of the expression plasmids. At 48 h after transfection, whole-cell lysates were immunoprecipitated with the anti-FLAG (a) or with anti-HA (b) antibody, followed by immunoblotting with the indicated antibodies. Aliquots of whole-cell lysates were subjected to immunoblotting with the anti-FLAG or with the anti-HA antibody to monitor the expression levels of FLAG-p73α, HA-p65 and HA-p50 (right panels). (c) Schematic drawing of the full-length p65 and the COOH-terminal deletion mutant, p65ΔC. RHD, Rel homology domain; NLS, nuclear localization signal; TAD, transactivation domain. (d) p65ΔC lacks the transcriptional activity. H1299 cells were co-transfected with the NF-κB-responsive luciferase reporter plasmid and pRL-TK *Renilla* luciferase cDNA together with the empty plasmid, HA-p65 plus HA-p50, HA-p65ΔC plus HA-p50 or HA-p65ΔC. At 48 h after transfection, the luciferase activities were measured. (e) Downregulation of p73α is induced by the full-length p65 but not by p65ΔC. H1299 cells were co-transfected with the expression plasmid for FLAG-p73α together with HA-p65 plus HA-p50 or HA-p65ΔC plus HA-p50. At 48 h post-transfection, whole-cell lysates were processed for immunoblotting with the indicated antibodies. Actin was used to confirm that an equivalent amount of protein was loaded into each lane.

performed the luciferase reporter assay. As shown in Figure 7d, HA-p65ΔC alone failed to drive transcription from the NF-κB luciferase reporter, whereas two- to three-fold increase in the luciferase activity was detectable in cells expressing exogenous HA-p65ΔC and HA-p50, which might be due to the complex formation between the endogenous p65 and HA-p50. We then examined the possible effects of HA-p65ΔC on the expression level of FLAG-p73α. H1299 cells were co-transfected with the indicated combinations of the expression plasmids, and whole-cell lysates were analysed for the expression level of FLAG-p73α by immunoblotting. As shown in Figure 7e, WT p65 significantly reduced the amount of FLAG-p73α, whereas HA-p65ΔC had an ability to stabilize FLAG-p73α. Collectively, these results strongly suggest that the transactivation property of NF-κB is required for the degradation of p73α.

Discussion

In the present study, we have found for the first time that NF-κB promotes the ubiquitin-dependent proteasomal turnover of p73 in the absence of a direct physical interaction between them, and also demonstrated that the transcriptional activity of NF-κB is required for this process. In contrast, NF-κB had negligible effects on p53 and p63. Thus, it is likely that the NF-κB-mediated degradation of p73 contributes to the protection of cells from p73-dependent apoptosis. To our knowledge, this is the first report describing the detailed properties of the NF-κB-dependent inhibitory mechanism of p73 function.

Genotoxic stresses increase the stability of p73 and enhance its proapoptotic activity in a pathway dependent on c-Abl (Agami *et al*., 1999; Gong *et al*., 1999; Yuan *et al*., 1999). Intriguingly, Kawai *et al*. (2002) reported that c-Abl phosphorylates IκBα at Tyr-305 to increase its stability, and thereby inhibiting the nuclear translocation and activation of NF-κB, suggesting that the inactivation of NF-κB contributes to the c-Abl-mediated apoptosis. Additionally, it has been demonstrated that, during the cisplatin-mediated apoptosis in hepatocellular carcinoma cells, the downregulation of NF-κB transcriptional activity is correlated with the accumulation of p73 (Kim *et al*., 2004). In contrast to the DNA-damaging agents that activate c-Abl, TNF-α treatment had undetectable effect on c-Abl (Kharbanda *et al*., 1995). According to our present results, the activation of the endogenous NF-κB induced by TNF-α resulted in a significant decrease in the stability of p73α. Taken together, it is likely that c-Abl plays an important role in the regulation of NF-κB-mediated destabilization of p73.

Since we could not detect the physical interaction between NF-κB and p73α, NF-κB might regulate p73α stability through an indirect mechanism. Deletion analysis revealed that p65ΔC fails to reduce the amount of p73α, raising a possibility that the transactivation function of NF-κB might be required for the degradation of p73α, and that there could exist an unidentified E3 ubiquitin ligase(s) among the direct targets of NF-κB. Recently, Rossi *et al.* (2005) described that an HECT-type E3 ubiquitin ligase Itch binds to p73, and promotes its degradation through the ubiquitin–proteasome pathway. In contrast, Itch had no detectable effect on p53. Additionally, it has been shown that Jun kinase regulates the TNF-α-mediated apoptosis through the activation of Itch (Chang *et al.*, 2006). Although the examination of the human *Itch* promoter region showed the presence of several putative DNA-binding sites of NF-κB, the enforced expression of NF-κB or TNF-α-mediated activation of the endogenous NF-κB failed to induce the endogenous *Itch* as examined by RT–PCR (data not shown). Considering that p53 is targeted for ubiquitination not only by MDM2 but also by Pirh2 (Leng *et al.*, 2003), it is likely that an as yet unidentified E3 ubiquitin ligase(s) distinct from Itch might be involved in the NF-κB-mediated degradation of p73α.

Among p53 family members, the NF-κB-mediated reduction was highly specific to p73α. The protein stability of p53, p73β and p63α was unaffected by the enforced expression of NF-κB. Lee and La Thangue (1999) described that p73β is much more stable than p73α, suggesting that the unique COOH-terminal extension of p73α is critical for its stability. Recently, we found that RanBPM binds to the extreme COOH-terminal region of p73α to inhibit its ubiquitination and thereby increasing its stability (Kramer *et al.*, 2005). However, RanBPM had undetectable effects on the stability of p53. Thus, it is possible that RanBPM might mask the p73α COOH-terminal lysine residues, which could be sites for ubiquitin ligation. Alternatively, the unique p73α COOH-terminal region could mediate the interaction with unknown cellular protein(s) required for the degradation of p73 induced by NF-κB. Of note, Wan and DeGregori (2003) found that NF-κB promotes T-cell survival by inhibiting the activation of p73 in response to antigenic stimulation. They described that NF-κB directly antagonizes the E2F-1-dependent upregulation of *p73* transcription. The interpretation that NF-κB inhibits the transcription of *p73* is contradicted by our present findings. In addition to the DNA-damage-induced stabilization of p73, p73 is regulated at mRNA level in response to certain apoptotic and differentiation stimuli. For example, p73 is transcriptionally induced by E2F-1 during the apoptotic response to T-cell receptor activation (Lissy *et al.*, 2000). Fontemaggi *et al.* (2001) found that *p73* mRNA is upregulated by E2F-1 during muscle, neuronal and monocytic differentiation. Therefore, it appears that employment of the NF-κB-dependent transcriptional or post-translational mechanism to downregulate p73 is dependent upon the types of stimulation and/or cell types. The propensity of cells to survive or die is determined by the balance between proapoptotic and prosurvival signals. In this connection, NF-κB-mediated degradation of p73 is a novel mechanism that regulates cell survival and death in response to a variety of cellular stresses.

Materials and methods

Cell culture and transfection

MEFs, and COS7 cells were grown in Dulbecco's modified Eagle's medium supplemented with 10% heat-inactivated fetal bovine serum (Invitrogen, Grand Island, NY, USA), 100 IU/ml penicillin and 100 μg/ml streptomycin. p53-deficient human lung carcinoma H1299 cells were cultured in RPMI 1640 medium supplemented with 10% heat-inactivated fetal bovine serum and antibiotic mixture. Cultures were maintained at 37°C in a water-saturated atmosphere of 5% CO_2 in air. For transfection, H1299 and COS7 cells were transfected with the indicated combinations of the expression plasmids using LipofectAMINE 2000 (Invitrogen) and FuGENE6 (Roche Molecular Biochemicals, Indianapolis, IN, USA), respectively.

Construction of the deletion mutant of p65

p65ΔC was generated by PCR-based strategy using the forward primer 5′-TAGAATTCGGGACGATCTGTTTCCC CTCATC-3′ and the reverse primer 5′-TTCTCGAGTTAAA GGACTGGGGCAGAGGACGG-3′. Underlined nucleotides were *Eco*RI and *Xho*I restriction sites. Amplified fragments were digested with *Eco*RI and *Xho*I, and subcloned into the identical restriction sites of pCMV-HA expression plasmid (Clontech Laboratories, Palo Alto, CA, USA) to give pCMV-HA-p65ΔC.

Immunoblotting

Cells were washed twice with phosphate-buffered saline (PBS), lysed in buffer containing 25 mM Tris-Cl, pH 8.0, 137 mM NaCl, 2.7 mM KCl, 1% Triton X-100 and protease inhibitor cocktail (Sigma Chemical Co., St Louis, MO, USA), and sonicated for 10 s followed by centrifugation at 15 000 r.p.m. for 10 min at 4°C to remove insoluble materials. Aliquots of whole-cell lysates (25–50 μg) were boiled in the SDS-sample buffer for 5 min, loaded onto 8% SDS–PAGE, and electrotransferred onto Immobilon-P membranes (Millipore, Bedford, MA, USA). The membranes were blocked with TBS-T (50 mM Tris-Cl, pH 8.0, 100 mM NaCl and 0.1% Tween-20) containing 5% nonfat dry milk, and then incubated at room temperature for 1 h with the monoclonal anti-FLAG (M2, Sigma Chemical Co.), monoclonal anti-HA (12CA5, Roche Molecular Biochemicals), monoclonal anti-p73 (Ab-4, NeoMarkers, Inc., Fremont, CA, USA), monoclonal anti-p53 (PAb1801, Santa Cruz Biotechnologies, Santa Cruz, CA, USA), monoclonal anti-p63 (Ab-1, NeoMarkers), polyclonal anti-p65 (C-20, Santa Cruz Biotechnologies), polyclonal anti-p50 (H-119, Santa Cruz Biotechnologies), or with polyclonal anti-actin (20–33, Sigma Chemical Co.) antibody, followed by an incubation with corresponding horseradish peroxidase-conjugated goat anti-mouse or anti-rabbit secondary antibody (Cell Signaling, Beverly, MA, USA) for 1 h at room temperature. Protein bands were finally detected by enhanced chemiluminescence detection system (Amersham Biosciences, Inc., Piscataway, NJ, USA).

Co-immunoprecipitation analysis
Equal amounts of whole-cell lysates were precleared with 30 μl of protein G-Sepharose (Amersham Bioscience). After centrifugation, the supernatant was incubated with the indicated antibodies at 4°C for 2 h. The immunocomplexes were then incubated with protein G-Sepharose beads at 4°C for 1 h, which were then pelleted by centrifugation at 15 000 r.p.m. for 5 min. The immunocomplexes were washed with the lysis buffer three times at 4°C, denatured with an equal volume of 2 × SDS-sample buffer, and analysed by immunoblotting with the desired primary antibodies.

RT–PCR
Total RNA was prepared by using RNeasy Mini Kit (Qiagen Inc., Valencia, CA, USA) according to the manufacturer's protocol. One microgram of total RNA was used to synthesize the first strand cDNA using random primers and a SuperScript II reverse transcriptase (Invitrogen). Reverse transcription was performed at 42°C for 1 h, and the reverse transcripts were amplified by standard PCR with rTaq DNA polymerase (Takara, Ohtsu, Japan). The primers used for PCR were as follows: *BAX*, 5′-TTTGCTTCAGGGTTTCATCC-3′ (sense) and 5′-CAGTTGAAGTTGCCGTCAGA-3′ (antisense); *GAPDH*, 5′-ACCTGACCTGCCGTCTAGAA-3′ (sense) and 5′-TCCACCACCCTGTTGCTGTA-3′ (antisense); *p73α*, 5′-TGGAACCAGACAGCACCTACTTCG-3′ (sense) and 5′-TGCTGGAAAGTGACCTCAAAGTGG-3′ (antisense).

Subcellular fractionation
Cells were washed twice with PBS, lysed in lysis buffer containing 10 mM Tris-HCl, pH 7.5, 1 mM EDTA, 0.5% Nonidet P-40, and protease inhibitor cocktail for 10 min at 4°C, and centrifuged at 3000 r.p.m. for 5 min at 4°C to separate the soluble (cytoplasmic) from the insoluble (nuclear) fraction. The insoluble fraction was washed completely with the lysis buffer and resuspended in buffer containing 25 mM Tris-Cl, pH 8.0, 137 mM NaCl, 2.7 mM KCl, 1% Triton X-100 and protease inhibitor cocktail. The nuclear and cytoplasmic fractions were then analysed by immunoblotting with monoclonal anti-Lamin B (Ab-1, Oncogene Reseach Products), or with monoclonal anti-α-tubulin antibody (Ab-2, NeoMarkers, Inc.).

Indirect immunofluorescence assay
H1299 cells were seeded onto the glass coverslips, and treated with TNF-α (20 ng/ml) or left untreated for 1 h cells were then fixed with 3.7% formaldehyde for 30 min at room temperature, and permeabilized with 0.2% Triton X-100 for 5 min at room temperature. After cells were blocked with 3% bovine serum albumin (BSA) for 1 h at room temperature, they were incubated with the polyclonal anti-p65 or with the polyclonal anti-p50 antibody for 1 h at room temperature. The primary antibodies were detected with FITC-conjugated secondary antibody (Invitrogen) for 1 h at room temperature. Cell nuclei were stained with 4′6-diamino-2-phenylindole (DAPI) (Sigma Chemical Co.), and cells were observed under a Fluoview laser scanning confocal microscope (Olympus, Tokyo, Japan).

Luciferase reporter assay
H1299 cells were co-transfected with 100 ng of the p53/p73-responsive luciferase reporter plasmid (*BAX* or *MDM2*), 10 ng of pRL-TK *Renilla* luciferase cDNA, and 25 ng of the expression plasmid for FLAG-p73α or FLAG-p53 together with or without the increasing amounts of HA-p65 and HA-p50 expression plasmids. At 48 h after transfection, cells were washed with PBS, and resuspended in passive lysis buffer (Promega Corp., Madison, WI, USA). Both firefly and *Renilla* luciferase activities were assayed with the dual-luciferase reporter assay system (Promega Corp.). The firefly luminescence signal was normalized based on the Renilla luminescence signal.

Protein decay rate analysis
COS7 cells were co-transfected with the indicated combinations of the expression plasmids. At 24 h after transfection, cells were treated with cycloheximide (Sigma Chemical Co.) at a final concentration of 100 μg/ml. At the indicated time points after the treatment with cycloheximide, cells were harvested, and whole-cell lysates were processed for immunoblot analysis with the anti-p73 or with the anti-actin antibody. Densitometry was used to quantify the amounts of FLAG-p73α which normalized to actin.

Ubiquitination assay
COS7 cells were co-transfected with the constant amount of FLAG-p73α and His-tagged ubiquitin, together with or without the increasing amounts of HA-p65 and HA-p50. At 48 h after transfection, cells were exposed to MG-132 (20 μM) for 6 h. Cells were then lysed in lysis buffer containing 6 M guanidine–HCl, 0.1 M Na_2HPO_4/NaH_2PO_4, pH 8.0 and 10 mM imidazole. Ubiquitinated materials were recovered by Ni^{2+}-NTA-agarose beads (Qiagen), and subsequently analysed by immunoblotting with the anti-p73 antibody.

FACS analysis
H1299 cells were co-transfected with indicated combinations of the expression plasmids. At 48 h after transfection, cells were washed twice with PBS, resuspended in 600 μl of a propidium iodide mixture containing 0.05% RNase, 0.25% Triton X-100 and 50 μg/ml of propidium iodide, and then incubated in the dark at 4°C for 30 min. Prior to performing FACS analysis, cells were filtered through a 40-μm nylon mesh. Cells were then analysed using the FACScan system (Becton Dickinson, Mountain View, CA, USA) in conjunction with CellQuest software (Becton Dickinson).

Colony formation assay
H1299 cells were co-transfected with indicated combinations of the expression plasmids. Total amount of plasmid DNA was kept constant (1 μg) with the empty plasmid. At 24 h after transfection, cells were selected with G418 (400 μg/ml) for 2 weeks. G418-resistant colonies were fixed in methanol, and stained with Giemsa's solution.

Abbreviations

CHX, cycloheximide; MEF, mouse embryonic fibroblasts; NF-κB, nuclear factor kappa B; TNF-α, tumor necrosis factor α; Ub, ubiquitin.

Acknowledgements

We thank members of our laboratory for helpful discussions. We also thank Y Nakamura for excellent technical assistance. We give special thanks to Dr M Karin for providing us with $p65^{-/-}$ MEF. This work was supported in part by a Grant-in-Aid from the Ministry of Health, Labour and Welfare for Third Term Comprehensive Control Research for Cancer, a Grant-in-Aid for Scientific Research on Priority Areas from the Ministry of Education, Culture, Sports, Science and Technology, Japan, and a Grant-in-Aid for Scientific Research from Japan Society for the Promotion of Science.